arXiv:1703.03841v1 [math.NA] 10 Mar 2017

Efficient Stochastic Asymptotic-Preserving IMEX Methods for Transport Equations with Diffusive Scalings and Random Inputs*

Shi Jin†, Hanqing Lu‡and Lorenzo Pareschi§

March 14, 2017

Abstract

For linear transport and radiative heat transfer equations with random inputs, we develop new generalized polynomial chaos based Asymptotic-Preserving stochastic Galerkin schemes that allow efficient computation for the problems that contain both uncertainties and multiple scales. Compared with previous methods for these problems, our new method use the implicit-explicit (IMEX) time discretization to gain higher order accuracy, and by using a modified diffusion operator based penalty method, a more relaxed stability condition–a hyperbolic, rather than parabolic, CFL stability condition, is achieved in the case of small mean free path in the diffusive regime. The stochastic Asymptotic-Preserving property of these methods will be shown asymptotically, and demonstrated numerically, along with computational cost comparison with previous methods.

Key words. Transport equation, radiative heat transfer, uncertainty, asymptotic preserving, diffusion limit, stochastic Galerkin, implicit-explicit Runge-Kutta methods.

Contents

1 Introduction **2**

2 The Linear Neutron Transport Equation with Random Inputs **3**
2.1 The gPC-SG Formulation 4
2.2 An Efficient IMEX Runge-Kutta Scheme 5
2.3 The Space Discretization 7
2.4 The sAP property 9

3 The Radiative Heat Transfer Equation with Random Inputs **11**
3.1 An Even-Odd Decomposition 12
3.2 The gPC-SG Formulation 12
3.3 An Efficient IMEX-RK Scheme 13
3.3.1 The IMEX Runge-Kutta Method 14
3.4 The sAP Property 16

*This research was supported by NSF grants DMS-1522184 and DMS-1107291: RNMS KI-Net, by NSFC grant No. 91330203, and by the Office of the Vice Chancellor for Research and Graduate Education at the University of Wisconsin, Madison, with funding from the Wisconsin Alumni Research Foundation. The research was partially supported by the research grant GNCS-INDAM 2016 *Numerical methods for uncertainty quantification in hyperbolic and kinetic equations.*

†Department of Mathematics, University of Wisconsin, Madison, WI 53706, USA (sjin@wisc.edu) and Institute of Natural Sciences, School of Mathematical Science, MOE-LSEC and SHL-MAC, Shanghai Jiao Tong University, Shanghai 200240, China.

‡Department of Mathematics, University of Wisconsin, Madison, WI 53706, USA (hanqing@math.wisc.edu).

§Department of Mathematics & Computer Science, University of Ferrara, Ferrara 44121, Italy (lorenzo.pareschi@unife.it).

4 Numerical Tests **17**
4.1 Test 1: The Linear Transport Equation 17
4.2 Test 2: The Linear Transport Equation with Random Inputs 18
4.3 Test 3: The Radiative Heat Transfer Equation 19
4.4 Test 4: The Radiative Heat Transfer Equation with Random Inputs 20

5 Conclusions **21**

1 Introduction

Transport equations, for example, linear transport equations and radiative transfer equations, arise in many important physical applications, from the microscopic neutron transport to large scale astrophysical problems [10]. As in general kinetic theory, one of the main challenges is its high dimensionality, since these equations describe particle density distributions defined in the phase space, with independent variables time, space and particle velocity. Another challenge is the multiscale nature, since the Knudsen number, the dimensionless mean free path, could vary in different orders of magnitude in the computational problems. When the Knudsen number is $O(1)$, we are in the kinetic regime. When it is small, usually one can approximate the kinetic equations by hydrodynamic or diffusion type equations which are macroscopic equations defined in physical space thus are much more efficient for numerical computations. Asymptotic-preserving (AP) schemes, which mimic the asymptotic transition from the kinetic to the macroscopic equation at the discrete level, have been proven to be an effective computational paradigm for such multiscale kinetic or transport equations, and have found many applications in kinetic theory [11, 12, 13, 16]. For those relevant to the equations to be studied in this article, see for example in neutron transport equations [2, 6, 14, 20, 22, 24, 26, 27, 28, 30], and nonlinear radiative transfer [5, 23, 34].

In this article, we are interested in addressing the third challenge in kinetic modeling: the *uncertainty*, for transport and radiative transfer equations. Since kinetic equations often arise from microscopic equations, for example Newton's second law or particle dynamics, via taking mean-field limits [4, 33], one often encounters difficulties in determining precisely or accurately terms such as collision kernels or scattering coefficients. In addition, initial, boundary data or forcing or source terms could also be measured inaccurately. Thus uncertainty is *intrinsic* in kinetic models that must be studied in order to assess the accuracy of kinetic models and validate and enhance the computational reliability of kinetic modelings.

While uncertainty quantification (UQ) has been a popular field of scientific computing in many areas of scientific and engineering research, its study for kinetic equations has been scarce. Only recently one sees some development of efficient numerical methods for kinetic equations with uncertainties [7, 15, 18, 19, 21, 35]. In particular, in [21], the notion of *stochastic Asymptotic-Preserving* (sAP) was introduced. For generalized polynomial chaos (gPC) based stochastic Galerkin (SG) methods, which are the methods to be used in this article to study the uncertainties, it requires an SG method for kinetic equations with uncertainty, as Knudsen number goes to zero, becomes a SG method for the macroscopic hydrodynamic or diffusion equations. This is the stochastic extension of the deterministic AP schemes. Moreover, as realized in [21], and subsequently in other kinetic equations [18, 19, 35], under the SG framework, one obtains a vectorized system of deterministic kinetic equations based on which the deterministic AP machinery can be easily utilized to develop sAP schemes for random kinetic equations. The gPC approach for uncertain kinetic equations is natural, and efficient, since kinetic equations typically preserve the regularity of the initial data in the random space [15, 17, 18, 29], thus one indeed obtains *spectral* accuracy in the random space, and then the sAP property allows one to use *Knudsen number independent* time step, mesh sizes and the order of polynomial degrees in the gPC method.

While sAP schemes have been developed for linear transport equation [17, 21] and radiative heat transfer equations [19] with uncertainties, in this article we aim to *improve the accuracy and efficiency* of these methods. Since the gPC-SG based numerical methods lead to much larger system of equations (compared to the original kinetic equations which are scalar equations), and the random variables that

describe the uncertainties often live in high dimension, more efficient numerical methods can help to significantly reduce the computational cost. To this aim, we will make two improvements. First, we utilize the implicit-explicit (IMEX) Ruge-Kutta (RK) time marching methods (see [2, 3, 31] and the references therein) in order to gain high order of accuracy in time discretization. Second, since these equations, due to high scattering rates, encounter diffusive regimes, a typical AP scheme based on explicit discretization of the convection term needs a parabolic type CFL stability condition $\Delta t = O(\Delta x^2)$, where Δt is the time step and Δx is the spatial mesh size. A fully implicit scheme will overcome this constraint, but will introduce algebraic difficulties when inverting the entire transport operator numerically. We use a diffusion operator penalized method introduced in [2], which allows to improve the CFL condition to a hyperbolic one $\Delta t = O(\Delta x)$. We modify the approach of [2] by replacing the microscopic probability density distribution in the penalty term by the macroscopic density, which further simplifies the inversion of the implicit terms.

The rest of the paper is organized as follows. We develop the gPC-SG based IMEX-RK sAP schemes for the random linear transport equation in Section 2 and the random radiative heat transfer equations in Section 3. Numerical tests can be found in Section 4 that verify the efficiency and sAP property of these methods. Some final considerations are reported in Section 5.

2 The Linear Neutron Transport Equation with Random Inputs

In this section we consider a one-dimensional linear neutron transport equation with random inputs. The randomness may come from the cross section, initial data and boundary data. Let $f(t, x, v, z)$ be the probability density distribution of particles at position $x \in D \subset \mathbb{R}$, time $t \in \mathbb{R}^+$ and depending on $v \in (-1, 1)$, which is the cosine of the angle between the particle velocity and position. $z \in I_z \subset \mathbb{R}^d (d \geq 1)$ is the random variable with compact support I_z. Then the one-dimensional transport equation is

$$\varepsilon \partial_t f + v \partial_x f = \frac{1}{\varepsilon} \left(\frac{\sigma_s}{2} \int_{-1}^{1} f(v') dv' - \sigma f \right) + \varepsilon Q, \tag{1}$$

where $\sigma = \sigma(x, z)$ is the total cross section and $\sigma_s = \sigma_s(x, z)$ is the scattering cross-section. Then the absorption coefficient $\sigma_A = \sigma_A(x, z)$ is defined by $\sigma_A = \frac{\sigma - \sigma_s}{\varepsilon^2}$. $Q = Q(x, z)$ is the source term and the small parameter ε is the mean free path. Without loss of generality, σ_A and Q are neglected in this study.

The well-known diffusion limit $\varepsilon \to 0$ of the one-dimensional deterministic transport equation is of the following form as [25, 1]:

$$\partial_t \rho = \partial_x \left(\frac{1}{3\sigma_s} \partial_x \rho \right), \tag{2}$$

where

$$\rho = \frac{1}{2} \int_{-1}^{1} f dv.$$

One can understand the diffusion limit of the transport equation with random inputs through the following even-odd decomposition [20]. First write equation (1) for $v > 0$:

$$\varepsilon \partial_t f(v) + v \partial_x f(v) = \frac{1}{\varepsilon} \left(\frac{\sigma_s}{2} \int_{-1}^{1} f(v') dv' - \sigma f(v) \right), \tag{3a}$$

$$\varepsilon \partial_t f(-v) - v \partial_x f(-v) = \frac{1}{\varepsilon} \left(\frac{\sigma_s}{2} \int_{-1}^{1} f(v') dv' - \sigma f(-v) \right). \tag{3b}$$

Now denote the even and odd parities

$$r(t, x, v, z) = \frac{1}{2}(f(t, x, v, z) + f(t, x, -v, z)), \tag{4a}$$

$$j(t, x, v, z) = \frac{1}{2\varepsilon}(f(t, x, v, z) - f(t, x, -v, z)). \tag{4b}$$

Then (3) becomes

$$\partial_t r + v\partial_x j = -\frac{\sigma_s}{\varepsilon^2}(r-\rho) \tag{5a}$$

$$\partial_t j + \frac{1}{\varepsilon^2} v\partial_x r = -\frac{1}{\varepsilon^2}\sigma_s j. \tag{5b}$$

As $\varepsilon \to 0^+$, (5) yields

$$r = \rho, \quad j = -\frac{v}{\sigma_s(x,z)}\partial_x r. \tag{6}$$

Substituting (6) into the first equation of (5) and integrating over $v \in [0,1]$, one gets the limiting diffusion equation with random inputs (2).

Based on this even-odd decomposition, Jin, Xiu and Zhu proposed a gPC-SG formulation for the linear transport equation (1) with random cross-section $\sigma_s(x,z)$. The Stochastic Asymptotic-Preserving (sAP) property is also introduced for this problem and shown both asymptotically and numerically for this framework [21]. See also [17] for a sharp regularity and sAP proof. However, a parabolic CFL condition $\Delta t = O(\Delta x^2)$ has to be satisfied for the fully discretized scheme in (5) since the scheme will become an *explicit* scheme for the limiting diffusion equation (2) as ε goes to 0.

Now we propose an efficient sAP method for system (5) by applying the IMEX Runge-Kutta scheme [2] to the gPC Galerkin formulation to get rid of the parabolic CFL condition. Our scheme will fasten the algorithm significantly especially for the vectorized system after the Galerkin projection and can be shown to be sAP.

2.1 The gPC-SG Formulation

To approximate the solution, we use the gPC expansion via an orthogonal polynomials series. That is, for random variable $z \in \mathbb{R}^d$, one seeks

$$r(t,x,v,z) \approx r_N(t,x,v,z) = \sum_{k=1}^{K} \hat{r}_k(t,x,v)\Phi_k(z), \tag{7a}$$

$$j(t,x,v,z) \approx j_N(t,x,v,z) = \sum_{k=1}^{K} \hat{j}_k(t,x,v)\Phi_k(z), \tag{7b}$$

where $\left\{\Phi_k(z), 1 \le k \le K, K = \binom{d+N}{d}\right\}$ are from $\mathbb{P}_N^d$, the d-variate orthogonal polynomials of degree up to $N \ge 1$, and orthonormal

$$\int_{I_z} \Phi_i(z)\Phi_j(z)\pi(z)dz = \delta_{ij},\ 1 \le i,j \le K = dim(\mathbb{P}_N^d). \tag{8}$$

Here $\pi(z)$ is the probability density function of z and $\delta_{i,j}$ the Kronecker delta function.

Now one inserts the approximation (7) into the governing equation (5) and enforces the residue to be orthogonal to the polynomial space spanned by$\{\Phi_1, \cdots, \Phi_K\}$. Then, one obtains a set of vectorized deterministic equations for $\hat{\mathbf{r}} = (\hat{r}_1, \cdots, \hat{r}_K)^T$ and $\hat{\mathbf{j}} = (\hat{j}_1, \cdots, \hat{j}_K)^T$:

$$\partial_t \hat{\mathbf{r}} + v\partial_x \hat{\mathbf{j}} = -\frac{1}{\varepsilon^2}\mathbf{S}(x)(\hat{\mathbf{r}} - \hat{\boldsymbol{\rho}}), \tag{9a}$$

$$\partial_t \hat{\mathbf{j}} + \frac{v}{\varepsilon^2}\partial_x \hat{\mathbf{r}} = -\frac{1}{\varepsilon^2}\mathbf{S}(x)\hat{\mathbf{j}}, \tag{9b}$$

where

$$\hat{\boldsymbol{\rho}}(x,t) = \langle \hat{\mathbf{r}} \rangle = \int_0^1 \hat{\mathbf{r}} dv,$$

and $\mathbf{S}(x) = (s_{ij}(x))_{1\le i,j\le K}$ is $K \times K$ symmetric and positive definite matrix with entries

$$s_{ij}(x) = \int_{I_z} \sigma_s(x,z)\Phi_i(z)\Phi_j(z)\pi(z)dz. \tag{10}$$

As $\varepsilon \to 0^+$,

$$\hat{\mathbf{r}} = \hat{\boldsymbol{\rho}}, \quad \hat{\mathbf{j}} = -v\mathbf{S}^{-1}\partial_x\hat{\mathbf{r}}. \tag{11}$$

Inserting above into (9a) and integrating over v, one can obtain:

$$\partial_t\hat{\boldsymbol{\rho}} = \frac{1}{3}\partial_x[\mathbf{S}^{-1}(x)\partial_x\hat{\boldsymbol{\rho}}]. \tag{12}$$

Remark 2.1. If one applies the gPC-SG formulation for the limiting diffusion equation (2) directly, one gets

$$\partial_t\hat{\boldsymbol{\rho}} = \frac{1}{3}\partial_x[\tilde{\mathbf{S}}(x)\partial_x\hat{\boldsymbol{\rho}}], \tag{13}$$

where $\tilde{\mathbf{S}}(x) = (\tilde{s}_{ij}(x))_{1\le i,j\le K}$ is a $K \times K$ symmetric and positive definite matrix with entries

$$\tilde{s}_{ij}(x) = \int_{I_z} \frac{1}{\sigma_s(x,z)}\Phi_i(z)\Phi_j(z)\pi(z)dz. \tag{14}$$

Though $\tilde{\mathbf{S}}$ and $\mathbf{S}^{-1}$ are different matrix, proof in [32] shows that $\tilde{\mathbf{S}}\partial_x\hat{\boldsymbol{\rho}}$ and $\mathbf{S}^{-1}\partial_x\hat{\boldsymbol{\rho}}$ are of spectral error.

2.2 An Efficient IMEX Runge-Kutta Scheme

Following [2], we consider a penalization approach to avoid the parabolic CFL condition of a standard AP scheme in the diffusion limit. By adding and subtracting the term $\frac{\mu}{3}\partial_x(\mathbf{S}^{-1}\partial_x\hat{\boldsymbol{\rho}})$ in (9a) and the term $\phi v\partial_x\hat{\mathbf{r}}$ in (9b), we reformulate the problem into an equivalent form:

$$\begin{aligned}\partial_t\hat{\mathbf{r}} &= \left[-v\partial_x\hat{\mathbf{j}} - \frac{\mu}{3}\partial_x(\mathbf{S}^{-1}\partial_x\hat{\boldsymbol{\rho}})\right] + \left[-\frac{1}{\varepsilon^2}\mathbf{S}(\hat{\mathbf{r}}-\hat{\boldsymbol{\rho}}) + \frac{\mu}{3}\partial_x(\mathbf{S}^{-1}\partial_x\hat{\boldsymbol{\rho}})\right] \\ &= f_1(\hat{\mathbf{r}},\hat{\mathbf{j}}) + f_2(\hat{\mathbf{r}}), \end{aligned} \tag{15a}$$

$$\partial_t\hat{\mathbf{j}} = -\phi v\partial_x\hat{\mathbf{r}} - \frac{1}{\varepsilon^2}\left(\mathbf{S}\hat{\mathbf{j}} + (1-\varepsilon^2\phi)v\partial_x\hat{\mathbf{r}}\right) = g_1(\hat{\mathbf{r}}) + g_2(\hat{\mathbf{r}},\hat{\mathbf{j}}), \tag{15b}$$

where

$$f_1(\hat{\mathbf{r}},\hat{\mathbf{j}}) = -v\partial_x\hat{\mathbf{j}} - \frac{\mu}{3}\partial_x(\mathbf{S}^{-1}\partial_x\hat{\boldsymbol{\rho}}), \tag{16a}$$

$$f_2(\hat{\mathbf{r}}) = -\frac{1}{\varepsilon^2}\mathbf{S}(x)(\hat{\mathbf{r}}-\hat{\boldsymbol{\rho}}) + \frac{\mu}{3}\partial_x(\mathbf{S}^{-1}\partial_x\hat{\boldsymbol{\rho}}), \tag{16b}$$

$$g_1(\hat{\mathbf{r}}) = -\phi v\partial_x\hat{\mathbf{r}}, \tag{16c}$$

$$g_2(\hat{\mathbf{r}},\hat{\mathbf{j}}) = -\frac{1}{\varepsilon^2}\left(\mathbf{S}\hat{\mathbf{j}} + (1-\varepsilon^2\phi)v\partial_x\hat{\mathbf{r}}\right). \tag{16d}$$

Here we choose $\mu = \mu(\varepsilon)$ such that

$$\begin{aligned}&\lim_{\varepsilon\to 0}\mu = 1, \\ &\mu = 0 \quad \text{if} \quad \varepsilon = O(1);\end{aligned} \tag{17}$$

and $\phi = \phi(\varepsilon)$ such that

$$0 \le \phi \le \frac{1}{\varepsilon^2}. \tag{18}$$

The restriction on ϕ guarantees the positivity of $\phi(\varepsilon)$ and $(1-\varepsilon^2\phi(\varepsilon))$ so the problem remains well-posed uniformly in ε. We make the same simple choice of ϕ as in [20]:

$$\phi(\varepsilon) = \min\left\{1, \frac{1}{\varepsilon^2}\right\}. \tag{19}$$

Remark 2.2. Compared to the penalty term $\mu v^2 \partial_x(\mathbf{S}^{-1}\partial_x \hat{\mathbf{r}})$ used in [2], our choice of the penalty term in (9a) is *independent* of v. So only one large tridiagonal matrix needs to be inverted later at each stage of the IMEX-RK scheme for the fully discretization instead of a series of large tridiagonal matrix (the number depends on the number of v used in the velocity discretization). This fastens the algorithm in practice without any loss of accuracy, especially for uncertain problems.

Now we apply an IMEX-RK scheme to system (15) where $(f_1, g_1)^T$ is evaluated explicitly and $(f_2, g_2)^T$ implicitly, then we obtain

$$\hat{\mathbf{r}}^{n+1} = \hat{\mathbf{r}}^n + \Delta t \sum_{k=1}^{s} \tilde{b}_k f_1(\hat{\mathbf{R}}^k, \hat{\mathbf{J}}^k) + \Delta t \sum_{k=1}^{s} b_k f_2(\hat{\mathbf{R}}^k), \tag{20a}$$

$$\hat{\mathbf{j}}^{n+1} = \hat{\mathbf{j}}^n + \Delta t \sum_{k=1}^{s} \tilde{b}_k g_1(\hat{\mathbf{R}}^k) + \Delta t \sum_{k=1}^{s} b_k g_2(\hat{\mathbf{R}}^k, \hat{\mathbf{J}}^k), \tag{20b}$$

where the internal stages are

$$\hat{\mathbf{R}}^k = \hat{\mathbf{r}}^n + \Delta t \sum_{l=1}^{k-1} \tilde{a}_{kl} f_1(\hat{\mathbf{R}}^l, \hat{\mathbf{J}}^l) + \Delta t \sum_{l=1}^{k} a_{kl} f_2(\hat{\mathbf{R}}^l), \tag{21a}$$

$$\hat{\mathbf{J}}^k = \hat{\mathbf{j}}^n + \Delta t \sum_{l=1}^{k-1} \tilde{a}_{kl} g_1(\hat{\mathbf{R}}^l) + \Delta t \sum_{l=1}^{k} a_{kl} g_2(\hat{\mathbf{R}}^l, \hat{\mathbf{J}}^l). \tag{21b}$$

It is obvious that the scheme is characterized by the $s \times s$ matrices

$$\tilde{A} = (\tilde{a}_{ij}), A = (a_{ij}) \tag{22}$$

and the vectors $\tilde{b}, b \in \mathbb{R}^s$, which can be represented by a double table tableau in the usual Butcher notation

$$\begin{array}{c|c} \tilde{c} & \tilde{A} \\ \hline & \tilde{b}^T \end{array}, \qquad \begin{array}{c|c} c & A \\ \hline & b^T \end{array}.$$

The coefficients $\tilde{c}$ and c depend on the explicit part of the scheme:

$$\tilde{c}_i = \sum_{j=1}^{i-1} \tilde{a}_{ij}, \quad c_i = \sum_{j=1}^{i} a_{ij}\,. \tag{23}$$

In the literature, there are two main different types of IMEX-RK schemes characterized by the structure of the matrix A. We are interested in the IMEX-RK method of type A (see [2]) where the matrix A is invertible, which is not sensitive to the initial data. Of course, other IMEX-RK may be used as well, we refer to [2] for further examples.

As an example, we list the SSP$(3, 3, 2)$ scheme, which is the second order IMEX scheme we are going to use in the numerical results:

$$\begin{array}{c|ccc} 0 & 0 & 0 & 0 \\ 1/2 & 1/2 & 0 & 0 \\ 1 & 1/2 & 1/2 & 0 \\ \hline & 1/3 & 1/3 & 1/3 \end{array}, \qquad \begin{array}{c|ccc} 1/4 & 1/4 & 0 & 0 \\ 1/4 & 0 & 1/4 & 0 \\ 1 & 1/3 & 1/3 & 1/3 \\ \hline & 1/3 & 1/3 & 1/3 \end{array}. \tag{24}$$

To obtain $\hat{\mathbf{R}}^k$ in each internal stage of (21), one needs the quantity $\hat{\mathbf{P}}^k = \langle \hat{\mathbf{R}}^k \rangle = \int_0^1 \hat{\mathbf{R}}^k dv$ in the implicit part $f_2(\hat{\mathbf{R}}_k)$. This quantity can be implemented by the following procedure. Suppose one has

computed $\hat{\mathbf{R}}^l$ for $l = 1, \cdots, k-1$, then according to (21a):

$$\begin{aligned}\hat{\mathbf{R}}^k &= \hat{\mathbf{r}}^n + \Delta t \sum_{l=1}^{k-1} \left[\tilde{a}_{kl} f_1(\hat{\mathbf{R}}^l, \hat{\mathbf{J}}^l) + a_{kl} f_2(\hat{\mathbf{R}}^l)\right] + \Delta t\, a_{kk} \left(-\frac{1}{\varepsilon^2}\mathbf{S}(x)(\hat{\mathbf{R}}^k - \hat{\mathbf{P}}^k) + \frac{\mu}{3}\partial_x(\mathbf{S}^{-1}\partial_x \hat{\mathbf{P}}^k)\right) \\ &= \overline{\hat{\mathbf{R}}}^{k-1} + \Delta t\, a_{kk} \left(-\frac{1}{\varepsilon^2}\mathbf{S}(x)(\hat{\mathbf{R}}^k - \hat{\mathbf{P}}^k) + \frac{\mu}{3}\partial_x(\mathbf{S}^{-1}\partial_x \hat{\mathbf{P}}^k)\right).\end{aligned} \tag{25}$$

Here $\overline{\hat{\mathbf{R}}}^{k-1}$ represents all contributions in (25) from the first $k-1$ stages. Now one takes $\langle\cdot\rangle$ on both sides of (25) so that $(\hat{\mathbf{R}}^k - \hat{\mathbf{P}}^k)$ is cancelled out on the right hand side and one can obtain $\hat{\mathbf{P}}^k$ from the following diffusion equation in implicit form:

$$\hat{\mathbf{P}}^k - \Delta t a_{kk} \frac{\mu}{3}\partial_x(\mathbf{S}^{-1}\partial_x \hat{\mathbf{P}}^k) = \langle \overline{\hat{\mathbf{R}}}^{k-1} \rangle. \tag{26}$$

Then it is plugged back to (21a) in order to compute $\hat{\mathbf{R}}^k$.

2.3 The Space Discretization

To obtain the second order accuracy, we apply the upwind TVD scheme in the explicit transport part and center difference for other second derivatives. During each internal stage (21),

$$\begin{aligned}\hat{\mathbf{R}}_i^k =& \hat{\mathbf{r}}_i^n + \Delta t \sum_{l=1}^{k-1} \tilde{a}_{kl} \left\{ -\frac{v}{2\Delta x}(\hat{\mathbf{J}}_{i+1}^l - \hat{\mathbf{J}}_{i-1}^l) + \frac{v\phi^{1/2}}{2\Delta x}(\hat{\mathbf{R}}_{i+1}^l - 2\hat{\mathbf{R}}_i^l + \hat{\mathbf{R}}_{i-1}^l) \right. \\ & - \frac{v\phi^{1/2}}{4}(\boldsymbol{\gamma}_i^l - \boldsymbol{\gamma}_{i-1}^l + \boldsymbol{\beta}_{i+1}^l - \boldsymbol{\beta}_i^l) \\ & \left. - \frac{\mu}{3\Delta x^2}\left[\mathbf{S}_{i+1/2}^{-1}(\hat{\mathbf{P}}_{i+1}^l - \hat{\mathbf{P}}_i^l) - \mathbf{S}_{i-1/2}^{-1}(\hat{\mathbf{P}}_i^l - \hat{\mathbf{P}}_{i-1}^l)\right]\right\} \\ & + \Delta t \sum_{l=1}^{k} a_{kl} \left\{ -\frac{1}{\varepsilon^2}\mathbf{S}_i(\hat{\mathbf{R}}_i^l - \hat{\mathbf{P}}_i^l) \right. \\ & \left. + \frac{\mu}{3\Delta x^2}\left[\mathbf{S}_{i+1/2}^{-1}(\hat{\mathbf{P}}_{i+1}^l - \hat{\mathbf{P}}_i^l) - \mathbf{S}_{i-1/2}^{-1}(\hat{\mathbf{P}}_i^l - \hat{\mathbf{P}}_{i-1}^l)\right]\right\},\end{aligned} \tag{27a}$$

$$\begin{aligned}\hat{\mathbf{J}}_i^k =& \hat{\mathbf{j}}_i^n + \Delta t \sum_{l=1}^{k-1} \tilde{a}_{kl} \left\{ -\frac{v\phi}{2\Delta x}(\hat{\mathbf{R}}_{i+1}^l - \hat{\mathbf{R}}_{i-1}^l) + \frac{v\phi^{1/2}}{2\Delta x}(\hat{\mathbf{J}}_{i+1}^l - 2\hat{\mathbf{J}}_i^l + \hat{\mathbf{J}}_{i-1}^l) \right. \\ & \left. - \frac{v\phi}{4}(\boldsymbol{\gamma}_i^l - \boldsymbol{\gamma}_{i-1}^l - \boldsymbol{\beta}_{i+1}^l + \boldsymbol{\beta}_i^l)\right\} \\ & - \Delta t \sum_{l=1}^{k} a_{kl} \frac{1}{\varepsilon^2} \left\{ \mathbf{S}_i \hat{\mathbf{J}}_i^l + (1 - \varepsilon^2\phi) v \frac{\hat{\mathbf{R}}_{i+1}^l - \hat{\mathbf{R}}_{i-1}^l}{2\Delta x} \right\},\end{aligned} \tag{27b}$$

where

$$\begin{aligned}\boldsymbol{\gamma}_i^l =& \frac{1}{\Delta x}\text{minmod}\left(\hat{\mathbf{R}}_{i+1}^l + \phi^{-1/2}\hat{\mathbf{J}}_{i+1}^l - \hat{\mathbf{R}}_i^l - \phi^{-1/2}\hat{\mathbf{J}}_i^l, \right. \\ & \left. \hat{\mathbf{R}}_i^l + \phi^{-1/2}\hat{\mathbf{J}}_i^l - \hat{\mathbf{R}}_{i-1}^l - \phi^{-1/2}\hat{\mathbf{J}}_{i-1}^l\right),\end{aligned} \tag{28a}$$

$$\begin{aligned}\boldsymbol{\beta}_i^l =& \frac{1}{\Delta x}\text{minmod}\left(\hat{\mathbf{R}}_{i+1}^l - \phi^{-1/2}\hat{\mathbf{J}}_{i+1}^l - \hat{\mathbf{R}}_i^l + \phi^{-1/2}\hat{\mathbf{J}}_i^l, \right. \\ & \left. \hat{\mathbf{R}}_i^l - \phi^{-1/2}\hat{\mathbf{J}}_i^l - \hat{\mathbf{R}}_{i-1}^l + \phi^{-1/2}\hat{\mathbf{J}}_{i-1}^l\right).\end{aligned} \tag{28b}$$

Since $\hat{\mathbf{P}}^k$ can be obtained by (26), one can get fully discretized $\hat{\mathbf{P}}_i^k$ as following:

$$\hat{\mathbf{P}}_i^k - \Delta t a_{kk}\frac{\mu}{3\Delta x^2}\left[\mathbf{S}_{i+1/2}^{-1}(\hat{\mathbf{P}}_{i+1}^k - \hat{\mathbf{P}}_i^k) - \mathbf{S}_{i-1/2}^{-1}(\hat{\mathbf{P}}_i^k - \hat{\mathbf{P}}_{i-1}^k)\right] = \langle \overline{\hat{\mathbf{R}}}_i^{k-1} \rangle. \tag{29}$$

By inverting a tridiagonal matrix, one can obtain $\hat{\mathbf{P}}_i^k$. Then using (29), the fully discretized $\hat{\mathbf{R}}_i^k$ is obtained and thus $\hat{\mathbf{J}}_i^k$ subsequently as following:

$$\begin{aligned}
\left(\mathbf{I} + \frac{a_{kk}\Delta t}{\varepsilon^2}\mathbf{S}_i\right)\hat{\mathbf{R}}_i^k =& \hat{\mathbf{r}}_i^n + \Delta t\sum_{l=1}^{k-1}\tilde{a}_{kl}\left\{-\frac{v}{2\Delta x}(\hat{\mathbf{J}}_{i+1}^l - \hat{\mathbf{J}}_{i-1}^l) + \frac{v\phi^{1/2}}{2\Delta x}(\hat{\mathbf{R}}_{i+1}^l - 2\hat{\mathbf{R}}_i^l + \hat{\mathbf{R}}_{i-1}^l)\right.\\
&- \frac{v\phi^{1/2}}{4}(\boldsymbol{\gamma}_i^l - \boldsymbol{\gamma}_{i-1}^l + \boldsymbol{\beta}_{i+1}^l - \boldsymbol{\beta}_i^l)\\
&\left.-\frac{\mu}{3\Delta x^2}\left[\mathbf{S}_{i+1/2}^{-1}(\hat{\mathbf{P}}_{i+1}^l - \hat{\mathbf{P}}_i^l) - \mathbf{S}_{i-1/2}^{-1}(\hat{\mathbf{P}}_i^l - \hat{\mathbf{P}}_{i-1}^l)\right]\right\}\\
&+ \Delta t\sum_{l=1}^{k-1}a_{kl}\left\{-\frac{1}{\varepsilon^2}\mathbf{S}_i(\hat{\mathbf{R}}_i^l - \hat{\mathbf{P}}_i^l)\right.\\
&\left.+\frac{\mu}{3\Delta x^2}\left[\mathbf{S}_{i+1/2}^{-1}(\hat{\mathbf{P}}_{i+1}^l - \hat{\mathbf{P}}_i^l) - \mathbf{S}_{i-1/2}^{-1}(\hat{\mathbf{P}}_i^l - \hat{\mathbf{P}}_{i-1}^l)\right]\right\}\\
&+ \Delta t a_{kk}\left\{\frac{1}{\varepsilon^2}\mathbf{S}_i\hat{\mathbf{P}}_i^k + \frac{\mu}{3\Delta x^2}\left[\mathbf{S}_{i+1/2}^{-1}(\hat{\mathbf{P}}_{i+1}^k - \hat{\mathbf{P}}_i^k)\right.\right.\\
&\left.\left.-\mathbf{S}_{i-1/2}^{-1}(\hat{\mathbf{P}}_i^k - \hat{\mathbf{P}}_{i-1}^k)\right]\right\},
\end{aligned} \tag{30a}$$

$$\begin{aligned}
\left(1 + \frac{a_{kk}\Delta t}{\varepsilon^2}\mathbf{S}_i\right)\hat{\mathbf{J}}_i^k =& \hat{\mathbf{j}}_i^n + \Delta t\sum_{l=1}^{k-1}\tilde{a}_{kl}\left\{-\frac{v\phi}{2\Delta x}(\hat{\mathbf{R}}_{i+1}^l - \hat{\mathbf{R}}_{i-1}^l) + \frac{v\phi^{1/2}}{2\Delta x}(\hat{\mathbf{J}}_{i+1}^l - 2\hat{\mathbf{J}}_i^l + \hat{\mathbf{J}}_{i-1}^l)\right.\\
&\left.-\frac{v\phi}{4}(\boldsymbol{\gamma}_i^l - \boldsymbol{\gamma}_{i-1}^l + \boldsymbol{\beta}_{i+1}^l - \boldsymbol{\beta}_i^l)\right\}\\
&- \Delta t\sum_{l=1}^{k-1}a_{kl}\frac{1}{\varepsilon^2}\left\{\mathbf{S}_i\hat{\mathbf{J}}_i^l + (1-\varepsilon^2\phi)v\frac{\hat{\mathbf{R}}_{i+1}^l - \hat{\mathbf{R}}_{i-1}^l}{2\Delta x}\right\}\\
&- \Delta t a_{kk}\left(\frac{1-\varepsilon^2\phi}{\varepsilon^2}\right)v\frac{\hat{\mathbf{R}}_{i+1}^k - \hat{\mathbf{R}}_{i-1}^k}{2\Delta x}.
\end{aligned} \tag{30b}$$

After calculating all $\hat{\mathbf{R}}_i^k$ and $\hat{\mathbf{J}}_i^k$ for $k = 1, \cdots, s$, one can update $\hat{\mathbf{r}}_i^{n+1}$ and $\hat{\mathbf{j}}_i^{n+1}$ in (20),

$$\begin{aligned}
\hat{\mathbf{r}}_i^{n+1} =& \hat{\mathbf{r}}_i^n + \Delta t\sum_{k=1}^{s}\tilde{b}_k\left\{-\frac{v}{2\Delta x}(\hat{\mathbf{J}}_{i+1}^k - \hat{\mathbf{J}}_{i-1}^k) + \frac{v\phi^{1/2}}{2\Delta x}(\hat{\mathbf{R}}_{i+1}^k - 2\hat{\mathbf{R}}_i^k + \hat{\mathbf{R}}_{i-1}^k)\right.\\
&- \frac{v\phi^{1/2}}{4}(\boldsymbol{\gamma}_i^k - \boldsymbol{\gamma}_{i-1}^k + \boldsymbol{\beta}_{i+1}^k - \boldsymbol{\beta}_i^k)\\
&\left.-\frac{\mu}{3\Delta x^2}\left[\mathbf{S}_{i+1/2}^{-1}(\hat{\mathbf{P}}_{i+1}^k - \hat{\mathbf{P}}_i^k) - \mathbf{S}_{i-1/2}^{-1}(\hat{\mathbf{P}}_i^k - \hat{\mathbf{P}}_{i-1}^k)\right]\right\}\\
&+ \Delta t\sum_{k=1}^{s}b_k\left\{-\frac{1}{\varepsilon^2}\mathbf{S}_i(\hat{\mathbf{R}}_i^k - \hat{\mathbf{P}}_i^k)\right.\\
&\left.+\frac{\mu}{3\Delta x^2}\left[\mathbf{S}_{i+1/2}^{-1}(\hat{\mathbf{P}}_{i+1}^k - \hat{\mathbf{P}}_i^k) - \mathbf{S}_{i-1/2}^{-1}(\hat{\mathbf{P}}_i^k - \hat{\mathbf{P}}_{i-1}^k)\right]\right\},
\end{aligned} \tag{31a}$$

$$\begin{aligned}
\hat{\mathbf{j}}_i^{n+1} =& \hat{\mathbf{j}}_i^n + \Delta t\sum_{k=1}^{s}\tilde{b}_k\left\{-\frac{v\phi}{2\Delta x}(\hat{\mathbf{R}}_{i+1}^k - \hat{\mathbf{R}}_{i-1}^k) + \frac{v\phi^{1/2}}{2\Delta x}(\hat{\mathbf{J}}_{i+1}^k - 2\hat{\mathbf{J}}_i^k + \hat{\mathbf{J}}_{i-1}^k)\right.\\
&\left.-\frac{v\phi}{4}(\boldsymbol{\gamma}_i^k - \boldsymbol{\gamma}_{i-1}^k + \boldsymbol{\beta}_{i+1}^k - \boldsymbol{\beta}_i^k)\right\}
\end{aligned}$$

$$- \Delta t \sum_{k=1}^{k} b_k \frac{1}{\varepsilon^2} \left\{ \mathbf{S}_i \hat{\mathbf{J}}_i^k + (1-\varepsilon^2\phi) v \frac{\hat{\mathbf{R}}_{i+1}^k - \hat{\mathbf{R}}_{i-1}^k}{2\Delta x} \right\}, \tag{31b}$$

where $\boldsymbol{\gamma}_i^k$ and $\boldsymbol{\beta}_i^k$ are defined the same as in (28).

We choose [2]

$$\mu = \exp(-\varepsilon^2/\Delta x). \tag{32}$$

Thus, for large value of ε, (e.g., $\varepsilon = 1$), one can avoid the loss of accuracy caused by adding and subtracting the penalty term; for very small value of ε, (e.g., $\varepsilon \to 0$), $\mu \to 1$.

Before continuing some observations are appropriate.

Remark 2.3.

- The velocity space is discretized by the so-called discrete ordinate method [8] which corresponds to use the Gauss-Legendre quadrature for the velocity integrals.
- Notice that the matrix $\mathbf{S}(x)$ can be precomputed. For each stage of (20), a large tridiagonal matrix has to be inverted. Since it is sparse and can be precomputed, fast algorithms can be applied.
- To get the boundary conditions for $\hat{\mathbf{r}}$ and $\hat{\mathbf{j}}$ we refer to [20] for details.

2.4 The sAP property

Denote

$$\begin{aligned}
f_1(\hat{\mathbf{R}}_i^l, \hat{\mathbf{J}}_i^l) =& -\frac{v}{2\Delta x}(\hat{\mathbf{J}}_{i+1}^l - \hat{\mathbf{J}}_{i-1}^l) + \frac{v\phi^{1/2}}{2\Delta x}(\hat{\mathbf{R}}_{i+1}^l - 2\hat{\mathbf{R}}_i^l + \hat{\mathbf{R}}_{i-1}^l) \\
& - \frac{v\phi^{1/2}}{4}(\boldsymbol{\gamma}_i^l - \boldsymbol{\gamma}_{i-1}^l + \boldsymbol{\beta}_{i+1}^l - \boldsymbol{\beta}_i^l) \\
& - \frac{\mu}{3\Delta x^2}\left[\mathbf{S}_{i+1/2}^{-1}(\hat{\mathbf{P}}_{i+1}^l - \hat{\mathbf{P}}_i^l) - \mathbf{S}_{i-1/2}^{-1}(\hat{\mathbf{P}}_i^l - \hat{\mathbf{P}}_{i-1}^l)\right], \\
f_2(\hat{\mathbf{R}}_i^l) =& -\frac{1}{\varepsilon^2}\mathbf{S}_i(\hat{\mathbf{R}}_i^l - \hat{\mathbf{P}}_i^l) \\
& + \frac{\mu}{3\Delta x^2}\left[\mathbf{S}_{i+1/2}^{-1}(\hat{\mathbf{P}}_{i+1}^l - \hat{\mathbf{P}}_i^l) - \mathbf{S}_{i-1/2}^{-1}(\hat{\mathbf{P}}_i^l - \hat{\mathbf{P}}_{i-1}^l)\right], \\
g_1(\hat{\mathbf{R}}_i^l) =& -\frac{v\phi}{2\Delta x}(\hat{\mathbf{R}}_{i+1}^l - \hat{\mathbf{R}}_{i-1}^l) + \frac{v\phi^{1/2}}{2\Delta x}(\hat{\mathbf{J}}_{i+1}^l - 2\hat{\mathbf{J}}_i^l + \hat{\mathbf{J}}_{i-1}^l) \\
& - \frac{v\phi}{4}(\boldsymbol{\gamma}_i^l - \boldsymbol{\gamma}_{i-1}^l - \boldsymbol{\beta}_{i+1}^l + \boldsymbol{\beta}_i^l), \\
g_2(\hat{\mathbf{R}}_i^l, \hat{\mathbf{J}}_i^l) =& \frac{1}{\varepsilon^2}\left[\mathbf{S}_i\hat{\mathbf{J}}_i^l + (1-\varepsilon^2\phi)v\frac{\hat{\mathbf{R}}_{i+1}^l - \hat{\mathbf{R}}_{i-1}^l}{2\Delta x}\right].
\end{aligned}$$

From (27) one gets

$$\begin{pmatrix} \hat{\mathbf{R}}_i^1 \\ \hat{\mathbf{R}}_i^2 \\ \vdots \\ \hat{\mathbf{R}}_i^s \end{pmatrix} = \begin{pmatrix} \hat{\mathbf{r}}_i^n \\ \hat{\mathbf{r}}_i^n \\ \vdots \\ \hat{\mathbf{r}}_i^n \end{pmatrix} + \Delta t \begin{pmatrix} 0 \\ \tilde{a}_{21} f_1(\hat{\mathbf{R}}_i^1, \hat{\mathbf{J}}_i^1) \\ \vdots \\ \sum_{l=1}^{s-1} \tilde{a}_{sl} f_1(\hat{\mathbf{R}}_i^l, \hat{\mathbf{J}}_i^l) \end{pmatrix} + \Delta t \mathbf{A} \begin{pmatrix} f_2(\hat{\mathbf{R}}_i^1) \\ f_2(\hat{\mathbf{R}}_i^2) \\ \vdots \\ f_2(\hat{\mathbf{R}}_i^s) \end{pmatrix}, \tag{33a}$$

$$\begin{pmatrix} \hat{\mathbf{J}}_i^1 \\ \hat{\mathbf{J}}_i^2 \\ \vdots \\ \hat{\mathbf{J}}_i^s \end{pmatrix} = \begin{pmatrix} \hat{\mathbf{j}}_i^n \\ \hat{\mathbf{j}}_i^n \\ \vdots \\ \hat{\mathbf{j}}_i^n \end{pmatrix} + \Delta t \begin{pmatrix} 0 \\ \tilde{a}_{21} g_1(\hat{\mathbf{R}}_i^1) \\ \vdots \\ \sum_{l=1}^{s-1} \tilde{a}_{sl} g_1(\hat{\mathbf{R}}_i^l) \end{pmatrix} + \Delta t \mathbf{A} \begin{pmatrix} g_2(\hat{\mathbf{R}}_i^1, \hat{\mathbf{J}}_i^1) \\ g_2(\hat{\mathbf{R}}_i^2, \hat{\mathbf{J}}_i^2) \\ \vdots \\ g_2(\hat{\mathbf{R}}_i^s, \hat{\mathbf{J}}_i^s) \end{pmatrix}, \tag{33b}$$

where

$$\mathbf{A}_{K(i-1)+1:Ki,K(j-1)+1:Kj} = A_{i,j}\mathbf{I}_{K\times K}, \quad \mathbf{I}_{K\times K} \text{ is the } K\times K \text{ identity matrix}, \tag{34}$$

and A is defined in (21). Denote $\mathbf{W}$ as the inverse matrix of $\mathbf{A}$, then one obtains from (33)

$$\Delta t \begin{pmatrix} f_2(\hat{\mathbf{R}}_i^1) \\ f_2(\hat{\mathbf{R}}_i^2) \\ \vdots \\ f_2(\hat{\mathbf{R}}_i^s) \end{pmatrix} = \mathbf{W}\left[\begin{pmatrix} \hat{\mathbf{R}}_i^1 \\ \hat{\mathbf{R}}_i^2 \\ \vdots \\ \hat{\mathbf{R}}_i^s \end{pmatrix} - \begin{pmatrix} \hat{\mathbf{r}}_i^n \\ \hat{\mathbf{r}}_i^n \\ \vdots \\ \hat{\mathbf{r}}_i^n \end{pmatrix} - \Delta t \begin{pmatrix} 0 \\ \tilde{a}_{21} f_1(\hat{\mathbf{R}}_i^1, \hat{\mathbf{J}}_i^1) \\ \vdots \\ \sum_{l=1}^{s-1} \tilde{a}_{sl} f_1(\hat{\mathbf{R}}_i^l, \hat{\mathbf{J}}_i^l) \end{pmatrix}\right], \tag{35a}$$

$$\Delta t \begin{pmatrix} g_2(\hat{\mathbf{R}}_i^1, \hat{\mathbf{J}}_i^1) \\ g_2(\hat{\mathbf{R}}_i^2, \hat{\mathbf{J}}_i^2) \\ \vdots \\ g_2(\hat{\mathbf{R}}_i^s, \hat{\mathbf{J}}_i^s) \end{pmatrix} = \mathbf{W}\left[\begin{pmatrix} \hat{\mathbf{J}}_i^1 \\ \hat{\mathbf{J}}_i^2 \\ \vdots \\ \hat{\mathbf{J}}_i^s \end{pmatrix} - \begin{pmatrix} \hat{\mathbf{j}}_i^n \\ \hat{\mathbf{j}}_i^n \\ \vdots \\ \hat{\mathbf{j}}_i^n \end{pmatrix} - \Delta t \begin{pmatrix} 0 \\ \tilde{a}_{21} g_1(\hat{\mathbf{R}}_i^1) \\ \vdots \\ \sum_{l=1}^{s-1} \tilde{a}_{sl} g_1(\hat{\mathbf{R}}_i^l) \end{pmatrix}\right], \tag{35b}$$

Since $\mathbf{W}$ has the same structure as $\mathbf{A}$, $\mathbf{W}$ should be a lower triangular matrix with entries

$$\mathbf{W}_{K(i-1)+1:Ki,K(j-1)+1:Kj} = \omega_{i,j}\mathbf{I}_{K\times K}, \tag{36}$$

where $W = (\omega_{i,j})$ is the inverse of the lower triangular matrix A in (21).

Then one can rewrite (35) as

$$\Delta t f_2(\hat{\mathbf{R}}_i^k) = \sum_{l=1}^{k} \omega_{kl}\left[\hat{\mathbf{R}}_i^l - \hat{\mathbf{r}}_i^n - \Delta t \sum_{l=1}^{k-1} \tilde{a}_{kl} f_1(\hat{\mathbf{R}}_i^l, \hat{\mathbf{J}}_i^l)\right], \tag{37a}$$

$$\Delta t g_2(\hat{\mathbf{R}}_i^k, \hat{\mathbf{J}}_i^k) = \sum_{l=1}^{k} \omega_{kl}\left[\hat{\mathbf{J}}_i^l - \hat{\mathbf{j}}_i^n - \Delta t \sum_{l=1}^{k-1} \tilde{a}_{kl} g_1(\hat{\mathbf{R}}_i^l)\right], \tag{37b}$$

More explicitly,

$$\begin{aligned}
&\Delta t\left\{-\frac{1}{\varepsilon^2}\mathbf{S}_i(\hat{\mathbf{R}}_i^k - \hat{\mathbf{P}}_i^k) + \frac{\mu}{3\Delta x^2}\left[\mathbf{S}_{i+1/2}^{-1}(\hat{\mathbf{P}}_{i+1}^k - \hat{\mathbf{P}}_i^k) - \mathbf{S}_{i-1/2}^{-1}(\hat{\mathbf{P}}_i^k - \hat{\mathbf{P}}_{i-1}^k)\right]\right\} \\
=&\sum_{l=1}^{k}\omega_{kl}\left\{\hat{\mathbf{R}}_i^l - \hat{\mathbf{r}}_i^n - \Delta t\sum_{l=1}^{k-1}\tilde{a}_{kl}\left[-\frac{v}{2\Delta x}(\hat{\mathbf{J}}_{i+1}^l - \hat{\mathbf{J}}_{i-1}^l) + \frac{v\phi^{1/2}}{2\Delta x}(\hat{\mathbf{R}}_{i+1}^l - 2\hat{\mathbf{R}}_i^l + \hat{\mathbf{R}}_{i-1}^l)\right.\right. \\
&\left.\left. -\frac{v\phi^{1/2}}{4}(\boldsymbol{\gamma}_i^l - \boldsymbol{\gamma}_{i-1}^l + \boldsymbol{\beta}_{i+1}^l - \boldsymbol{\beta}_i^l) - \frac{\mu}{3\Delta x^2}\left(\mathbf{S}_{i+1/2}^{-1}(\hat{\mathbf{P}}_{i+1}^l - \hat{\mathbf{P}}_i^l) - \mathbf{S}_{i-1/2}^{-1}(\hat{\mathbf{P}}_i^l - \hat{\mathbf{P}}_{i-1}^l)\right)\right]\right\},
\end{aligned} \tag{38a}$$

$$\begin{aligned}
&\Delta t\left\{\frac{1}{\varepsilon^2}\left[\mathbf{S}_i\hat{\mathbf{J}}_i^k + (1-\varepsilon^2\phi)v\frac{\hat{\mathbf{R}}_{i+1}^k - \hat{\mathbf{R}}_{i-1}^k}{2\Delta x}\right]\right\} \\
=&\sum_{l=1}^{k}\omega_{kl}\left\{\hat{\mathbf{J}}_i^l - \hat{\mathbf{j}}_i^n - \Delta t\sum_{l=1}^{k-1}\tilde{a}_{kl}\left[-\frac{v\phi}{2\Delta x}(\hat{\mathbf{R}}_{i+1}^l - \hat{\mathbf{R}}_{i-1}^l) + \frac{v\phi^{1/2}}{2\Delta x}(\hat{\mathbf{J}}_{i+1}^l - 2\hat{\mathbf{J}}_i^l + \hat{\mathbf{J}}_{i-1}^l)\right.\right. \\
&\left.\left. -\frac{v\phi}{4}(\boldsymbol{\gamma}_i^l - \boldsymbol{\gamma}_{i-1}^l - \boldsymbol{\beta}_{i+1}^l + \boldsymbol{\beta}_i^l)\right]\right\}.
\end{aligned} \tag{38b}$$

Thus, setting $\varepsilon \to 0$, since $\mathbf{S}_i$ is non-singular, one obtains

$$\hat{\mathbf{R}}_i^k = \hat{\mathbf{P}}_i^k, \tag{39a}$$

$$\hat{\mathbf{J}}_i^k = -v\mathbf{S}_i^{-1}\frac{\hat{\mathbf{R}}_{i+1}^k - \hat{\mathbf{R}}_{i-1}^k}{2\Delta x}. \tag{39b}$$

Inserting this back to (31a) and letting $\varepsilon \to 0$,

$$\hat{\mathbf{r}}_i^{n+1} = \hat{\mathbf{r}}_i^n + \Delta t \sum_{k=1}^{s} \tilde{b}_k \hat{f}_1(\hat{\mathbf{R}}_i^k) + \Delta t \sum_{k=1}^{s} b_k \hat{f}_2(\hat{\mathbf{R}}_i^k), \tag{40}$$

where

$$\hat{f}_1(\hat{\mathbf{R}}_i^k) = v^2 \frac{1}{4\Delta x^2} \left[\mathbf{S}_{i+1}^{-1}(\hat{\mathbf{R}}_{i+2}^k - \hat{\mathbf{R}}_i^k) - \mathbf{S}_{i-1}^{-1}(\hat{\mathbf{R}}_i^k - \hat{\mathbf{R}}_{i-2}^k) \right] \tag{41a}$$

$$- \frac{1}{3\Delta x^2} \left[\mathbf{S}_{i+1/2}^{-1}(\hat{\mathbf{R}}_{i+1}^k - \hat{\mathbf{R}}_i^k) - \mathbf{S}_{i-1/2}^{-1}(\hat{\mathbf{R}}_i^k - \hat{\mathbf{R}}_{i-1}^k) \right], \tag{41b}$$

$$\hat{f}_2(\hat{\mathbf{R}}_i^k) = \frac{1}{3\Delta x^2} \left[\mathbf{S}_{i+1/2}^{-1}(\hat{\mathbf{R}}_{i+1}^k - \hat{\mathbf{R}}_i^k) - \mathbf{S}_{i-1/2}^{-1}(\hat{\mathbf{R}}_i^k - \hat{\mathbf{R}}_{i-1}^k) \right]. \tag{41c}$$

Integrating above over v, one gets

$$\hat{\boldsymbol{\rho}}_i^{n+1} = \hat{\boldsymbol{\rho}}_i^n + \frac{\Delta t}{3\Delta x^2} \sum_{k=1}^{s} b_k \left[\mathbf{S}_{i+1/2}^{-1}(\hat{\mathbf{P}}_{i+1}^k - \hat{\mathbf{P}}_i^k) - \mathbf{S}_{i-1/2}^{-1}(\hat{\mathbf{P}}_i^k - \hat{\mathbf{P}}_{i-1}^k) \right] + O(\Delta x^2), \tag{42}$$

where

$$\hat{\mathbf{P}}_i^k = \hat{\boldsymbol{\rho}}_i^n + \frac{\Delta t}{3\Delta x^2} \sum_{l=1}^{k} a_{kl} \left[\mathbf{S}_{i+1/2}^{-1}(\hat{\mathbf{P}}_{i+1}^l - \hat{\mathbf{P}}_i^l) - \mathbf{S}_{i-1/2}^{-1}(\hat{\mathbf{P}}_i^l - \hat{\mathbf{P}}_{i-1}^l) \right], \tag{43}$$

which is an *implicit* RK scheme (requiring inverting a tridiagonal matrix at each stage) for the limiting diffusion equation (12) and also corresponds to (29). Thus, the sAP property [21] of the efficient IMEX R-K scheme is shown.

3 The Radiative Heat Transfer Equation with Random Inputs

Let $x \in D \subset \mathbb{R}^3$ be the space variable, $\Omega \in S^2$ be the direction variable, S^2 the unit sphere of $\mathbb{R}^3$, $z \in \mathbb{R}^d (d \geq 1)$ be the random variable and $t \in \mathbb{R}^+$ the time.

We denote by $I = I(x, \Omega, z, t)$ the radiative intensity and by $\theta(x, z, t)$ the material temperature. Introducing the Knudsen number ε, the radiative heat transfer equations in nondimensional form are

$$\varepsilon^2 M \partial_t I + \varepsilon \Omega \cdot \nabla_x I = B(\theta) - I \tag{44a}$$

$$\varepsilon^2 \partial_t \theta = \varepsilon^2 \Delta_x \theta - (B(\theta) - \langle I \rangle) \tag{44b}$$

with the total intensity

$$\langle I \rangle(x, z, t) = \frac{1}{|S|^2} \int_{S^2} I(x, \Omega, z, t) d\Omega, \tag{45}$$

and the black body intensity

$$B(\theta) = \sigma \theta^4, \tag{46}$$

where M is the Mach number ($= 1$ for this paper) and $\sigma = \sigma(x, z) > 0$ is the cross-section depending on the space variable and the random variable.

The initial conditions and reflection transmission boundary conditions are prescribed as following:

$$\begin{aligned} &I.C. \begin{cases} I(x, \Omega, z, 0) = I_I(x, \Omega, z), \\ \theta(x, z, 0) = \theta_I(x, z) \end{cases} \\ &B.C. \begin{cases} I(\hat{x}, \Omega, z, t) = \alpha(n(\hat{x}) \cdot \Omega) I(\hat{x}, \Omega', z, t) + [1 - \alpha(n(\hat{x}) \cdot \Omega)] I_B(\hat{x}, \Omega, z, t), \\ \qquad\qquad \text{for } n(\hat{x}) \cdot \Omega < 0 \\ \theta(\hat{x}, z, t) = \theta_B(\hat{x}, z, t) \end{cases} \end{aligned} \tag{47}$$

where $\hat{x} \in \partial D$ with outward unit normal $n(\hat{x})$ and $\Omega' = \Omega - 2n(\hat{x})(n(\hat{x}) \cdot \Omega)$ is the reflection of Ω on the tangent plane to ∂D. The reflectivity $\alpha,\ 0 \leq \alpha \leq 1$, depends on the incidence angle.

3.1 An Even-Odd Decomposition

For simplicity, we consider the one-dimensional case $x \in [0,1]$ and define $v = \cos(\Omega \cdot x), v \in [-1,1]$. Thus, the angular averaging is defined as:

$$\langle f \rangle = \frac{1}{2}\int_{-1}^{1} f(v)dv.$$

The one-dimensional radiative heat transfer equation is

$$\varepsilon^2 \partial_t I + \varepsilon v \partial_x I = B(\theta) - I \tag{48a}$$

$$\varepsilon^2 \partial_t \theta = \varepsilon^2 \partial_{xx}\theta - (B(\theta) - \langle I \rangle) \tag{48b}$$

For $v > 0$,

$$\begin{aligned} &\varepsilon^2 \partial_t I(v) + \varepsilon v \partial_x I(v) = B(\theta) - I(v) \\ &\varepsilon^2 \partial_t I(-v) - \varepsilon v \partial_x I(-v) = B(\theta) - I(-v) \\ &\varepsilon^2 \partial_t \theta = \varepsilon^2 \partial_{xx}\theta - (B(\theta) - \langle I \rangle) \end{aligned} \tag{49}$$

Now denote the even and odd parities

$$\begin{aligned} r(t,x,v,z) &= \frac{1}{2}(I(t,x,v,z) + I(t,x,-v,z)), \\ j(t,x,v,z) &= \frac{1}{2\varepsilon}(I(t,x,v,z) - I(t,x,-v,z)). \end{aligned} \tag{50}$$

Then (49) becomes

$$\partial_t r + v\partial_x j = \frac{1}{\varepsilon^2}(B(\theta) - r), \tag{51a}$$

$$\partial_t j + \frac{1}{\varepsilon^2} v \partial_x r = -\frac{1}{\varepsilon^2} j, \tag{51b}$$

$$\partial_t \theta = \partial_{xx}\theta - \frac{1}{\varepsilon^2}(B(\theta) - \langle r \rangle). \tag{51c}$$

As $\varepsilon \to 0$, (51) gives

$$B(\theta) = r = \langle r \rangle, \quad j = -v\partial_x r. \tag{52}$$

Applying this in (51a), integrating over v and adding to (51c)

$$\partial_t(\theta + B(\theta)) = \partial_x \left[\partial_x \theta + \frac{1}{3}\partial_x B(\theta)\right], \tag{53}$$

which is the same limiting diffusion equation one can derive from the Hilbert expansion as [23].

3.2 The gPC-SG Formulation

Now we deal with the uncertainty. Using gPC approximation for $r(t,x,v,z), j(t,x,v,z)$ and $\theta(t,x,z)$ and truncate at the N-th order,

$$r(t,x,v,z) \approx r_N(t,x,v,z) = \sum_{k=1}^{K} \hat{r}_k(t,x,v)\Phi_k(z) = \hat{\mathbf{r}} \cdot \mathbf{\Phi}, \tag{54a}$$

$$j(t,x,v,z) \approx j_N(t,x,v,z) = \sum_{k=1}^{K} \hat{j}_k(t,x,v)\Phi_k(z) = \hat{\mathbf{j}} \cdot \mathbf{\Phi}, \tag{54b}$$

$$\theta(t,x,z) \approx \theta_N(t,x,z) = \sum_{k=1}^{K} \hat{\theta}_k(t,x)\Phi_k(z) = \hat{\boldsymbol{\theta}} \cdot \mathbf{\Phi}, \tag{54c}$$

where Φ_k is the same as defined in (8) and

$$\hat{\boldsymbol{r}} = (\hat{r}_1, \hat{r}_2, \cdots, \hat{r}_K)^T, \tag{55a}$$
$$\hat{\boldsymbol{j}} = (\hat{j}_1, \hat{j}_2, \cdots, \hat{j}_K)^T, \tag{55b}$$
$$\hat{\boldsymbol{\theta}} = (\hat{\theta}_1, \hat{\theta}_2, \cdots, \hat{\theta}_K)^T, \tag{55c}$$
$$\hat{\boldsymbol{\Phi}} = (\hat{\Phi}_1, \hat{\Phi}_2, \cdots, \hat{\Phi}_K)^T. \tag{55d}$$

Then (51) becomes

$$\partial_t \hat{\mathbf{r}} + v\partial_x \hat{\mathbf{j}} = \frac{1}{\varepsilon^2}(\mathbf{B}(\hat{\boldsymbol{\theta}}) - \hat{\mathbf{r}}), \tag{56a}$$
$$\partial_t \hat{\mathbf{j}} + \frac{1}{\varepsilon^2} v\partial_x \hat{\mathbf{r}} = -\frac{1}{\varepsilon^2}\hat{\mathbf{j}}, \tag{56b}$$
$$\partial_t \hat{\boldsymbol{\theta}} = \partial_{xx}\hat{\boldsymbol{\theta}} - \frac{1}{\varepsilon^2}(\mathbf{B}(\hat{\boldsymbol{\theta}}) - \langle \hat{\mathbf{r}} \rangle). \tag{56c}$$

where $\mathbf{B}(\hat{\boldsymbol{\theta}}) = (B_j)_{1\le j\le K}$ with

$$B_j = \int_{I_z} (\hat{\boldsymbol{\theta}} \cdot \boldsymbol{\Phi})^4 \sigma(x,z)\Phi_j(z)\pi(z)dz \tag{57}$$

Similarly, the limiting diffusion equation (53) becomes

$$\partial_t[\hat{\boldsymbol{\theta}} + \mathbf{B}(\hat{\boldsymbol{\theta}})] = \partial_x \left[(\mathbf{I} + \frac{4}{3}\mathbf{C})\partial_x \hat{\boldsymbol{\theta}} \right], \tag{58}$$

where $\mathbf{I}$ is a $K \times K$ identity matrix and $\mathbf{C}(\hat{\boldsymbol{\theta}}) = (c_{ij})_{1\le i,j\le K}$ with

$$c_{ij} = \int_{I_z} (\hat{\boldsymbol{\theta}} \cdot \boldsymbol{\Phi})^3 \sigma(x,z)\Phi_i(z)\Phi_j(z)\pi(z)dz \tag{59}$$

The well-posedness of this equation under some gentle condition is proved in [19].

3.3 An Efficient IMEX-RK Scheme

One could apply the same relaxation method as in [20] for the system (56), but it will still suffer from the parabolic CFL condition $\Delta t = O(\Delta x^2)$. So similar as in section 2.2, we rewrite (56) as following

$$\partial_t \hat{\mathbf{r}} = -v\partial_x \hat{\mathbf{j}} + \frac{1}{\varepsilon^2}(\mathbf{B}(\hat{\boldsymbol{\theta}}) - \hat{\mathbf{r}}), \tag{60a}$$
$$\partial_t \hat{\mathbf{j}} = -\frac{1}{\varepsilon^2}(\hat{\mathbf{j}} + v\partial_x \hat{\mathbf{r}}), \tag{60b}$$
$$\partial_t \hat{\boldsymbol{\theta}} = \partial_{xx}\hat{\boldsymbol{\theta}} - \frac{1}{\varepsilon^2}(\mathbf{B}(\hat{\boldsymbol{\theta}}) - \langle \hat{\mathbf{r}} \rangle). \tag{60c}$$

By adding and subtracting the term $\frac{\mu}{3}\partial_{xx}\mathbf{B}(\hat{\boldsymbol{\theta}})$ in (60a) and the term $\phi v\partial_x \hat{\mathbf{r}}$ in (60b), we reformulate the problem into its equivalent form:

$$\begin{aligned}\partial_t \hat{\mathbf{r}} &= \left[-v\partial_x \hat{\mathbf{j}} - \frac{\mu}{3}\partial_{xx}\mathbf{B}(\hat{\boldsymbol{\theta}}) \right] + \left[\frac{1}{\varepsilon^2}(\mathbf{B}(\hat{\boldsymbol{\theta}}) - \hat{\mathbf{r}}) + \frac{\mu}{3}\partial_{xx}\mathbf{B}(\hat{\boldsymbol{\theta}}) \right], \\ &= f_1(\hat{\mathbf{j}}, \hat{\boldsymbol{\theta}}) + f_2(\hat{\mathbf{r}}, \hat{\boldsymbol{\theta}}),\end{aligned} \tag{61a}$$
$$\partial_t \hat{\mathbf{j}} = -v\phi\partial_x \hat{\mathbf{r}} - \frac{1}{\varepsilon^2}[\hat{\mathbf{j}} + (1-\varepsilon^2\phi)v\partial_x \hat{\mathbf{r}}] = g_1(\hat{\mathbf{r}}) + g_2(\hat{\mathbf{r}}, \hat{\mathbf{j}}), \tag{61b}$$

$$\partial_t \hat{\boldsymbol{\theta}} = \partial_{xx}\hat{\boldsymbol{\theta}} - \frac{1}{\varepsilon^2}(\mathbf{B}(\hat{\boldsymbol{\theta}}) - \langle \hat{\mathbf{r}} \rangle) = h(\hat{\boldsymbol{\theta}}), \tag{61c}$$

where

$$f_1(\hat{\mathbf{j}}, \hat{\boldsymbol{\theta}}) = -v\partial_x \hat{\mathbf{j}} - \frac{\mu}{3}\partial_{xx}\mathbf{B}(\hat{\boldsymbol{\theta}}), \tag{62a}$$

$$f_2(\hat{\mathbf{r}}, \hat{\boldsymbol{\theta}}) = \frac{1}{\varepsilon^2}(\mathbf{B}(\hat{\boldsymbol{\theta}}) - \hat{\mathbf{r}}) + \frac{\mu}{3}\partial_{xx}\mathbf{B}(\hat{\boldsymbol{\theta}}), \tag{62b}$$

$$g_1(\hat{\mathbf{r}}) = -v\phi\partial_x \hat{\mathbf{r}}, \tag{62c}$$

$$g_2(\hat{\mathbf{r}}, \hat{\mathbf{j}}) = -\frac{1}{\varepsilon^2}[\hat{\mathbf{j}} + (1 - \varepsilon^2\phi)v\partial_x \hat{\mathbf{r}}]. \tag{62d}$$

The constant μ and ϕ are chosen the same as in (17) and (19) respectively.

3.3.1 The IMEX Runge-Kutta Method

Now we apply an IMEX-RK scheme to system (61) where $(f_1, g_1, 0)^T$ is evaluated explicitly and $(f_2, g_2, h)^T$ implicitly, then we obtain

$$\hat{\mathbf{r}}^{n+1} = \hat{\mathbf{r}}^n + \Delta t \sum_{k=1}^{s} \tilde{b}_k f_1(\hat{\mathbf{J}}^k, \hat{\boldsymbol{\Theta}}^k) + \Delta t \sum_{k=1}^{s} b_k f_2(\hat{\mathbf{R}}^k, \hat{\boldsymbol{\Theta}}^k), \tag{63a}$$

$$\hat{\mathbf{j}}^{n+1} = \hat{\mathbf{j}}^n + \Delta t \sum_{k=1}^{s} \tilde{b}_k g_1(\hat{\mathbf{R}}^k) + \Delta t \sum_{k=1}^{s} b_k g_2(\hat{\mathbf{R}}^k, \hat{\mathbf{J}}^k), \tag{63b}$$

$$\hat{\boldsymbol{\theta}}^{n+1} = \hat{\boldsymbol{\theta}}^n + \Delta t \sum_{k=1}^{s} b_k h(\hat{\boldsymbol{\Theta}}^k), \tag{63c}$$

where the internal stages are

$$\hat{\mathbf{R}}^k = \hat{\mathbf{r}}^n + \Delta t \sum_{l=1}^{k-1} \tilde{a}_{kl} f_1(\hat{\mathbf{J}}^l, \hat{\boldsymbol{\Theta}}^l) + \Delta t \sum_{l=1}^{k} a_{kl} f_2(\hat{\boldsymbol{R}}^l, \hat{\boldsymbol{\Theta}}^l), \tag{64a}$$

$$\hat{\mathbf{J}}^k = \hat{\mathbf{j}}^n + \Delta t \sum_{l=1}^{k-1} \tilde{a}_{kl} g_1(\hat{\mathbf{R}}^l) + \Delta t \sum_{l=1}^{k} a_{kl} g_2(\hat{\mathbf{R}}^l, \hat{\mathbf{J}}^l), \tag{64b}$$

$$\hat{\boldsymbol{\Theta}}^k = \hat{\boldsymbol{\theta}}^n + \Delta t \sum_{l=1}^{k} a_{kl} h(\hat{\boldsymbol{\Theta}}^l). \tag{64c}$$

Notice that for each internal stage, one has to compute $\hat{\boldsymbol{\Theta}}_k$ first. Then $\hat{\mathbf{R}}_k$ and $\hat{\mathbf{J}}_k$ can be solved similarly as before.

$$\hat{\boldsymbol{\Theta}}^k = \hat{\boldsymbol{\theta}}^n + \Delta t \sum_{l=1}^{k} a_{kl} \left(\partial_{xx}\hat{\boldsymbol{\Theta}}^l - \frac{1}{\varepsilon^2}(\mathbf{B}(\hat{\boldsymbol{\Theta}}^l) - \langle \hat{\boldsymbol{R}}^l \rangle) \right). \tag{65}$$

Take $\langle \cdot \rangle$ on (64a),

$$\begin{aligned} \langle \hat{\mathbf{R}}^k \rangle =& \langle \hat{\mathbf{r}}^n + \Delta t \sum_{l=1}^{k-1} \tilde{a}_{kl} f_1(\hat{\mathbf{J}}^l, \hat{\boldsymbol{\Theta}}^l) + \Delta t \sum_{l=1}^{k-1} a_{kl} f_2(\hat{\mathbf{R}}^l, \hat{\boldsymbol{\Theta}}^l) \rangle + \Delta t a_{kk} \langle f_2(\hat{\mathbf{R}}^k, \hat{\boldsymbol{\Theta}}^k) \rangle \\ =& \langle \hat{\mathbf{r}}^n + \Delta t \sum_{l=1}^{k-1} \tilde{a}_{kl} f_1(\hat{\mathbf{J}}^l, \hat{\boldsymbol{\Theta}}^l) + \Delta t \sum_{l=1}^{k-1} a_{kl} f_2(\hat{\mathbf{R}}^l, \hat{\boldsymbol{\Theta}}^l) \rangle \\ &+ \Delta t a_{kk} \left(\frac{1}{\varepsilon^2}(\mathbf{B}(\hat{\boldsymbol{\Theta}}^k) - \langle \hat{\mathbf{R}}^k \rangle) + \frac{\mu}{3}\partial_{xx}\mathbf{B}(\hat{\boldsymbol{\Theta}}^k) \right). \end{aligned} \tag{66}$$

Add (65) and (66),

$$\begin{aligned}\hat{\boldsymbol{\Theta}}^k + \langle \hat{\mathbf{R}}^k \rangle =& \hat{\boldsymbol{\theta}}^n + \Delta t \sum_{l=1}^{k-1} a_{kl} h(\hat{\boldsymbol{\Theta}}^l) \\ &+ \langle \hat{\mathbf{r}}^n + \Delta t \sum_{l=1}^{k-1} \tilde{a}_{kl} f_1(\hat{\mathbf{J}}^l, \hat{\boldsymbol{\Theta}}^l) + \Delta t \sum_{l=1}^{k-1} a_{kl} f_2(\hat{\mathbf{R}}^l, \hat{\boldsymbol{\Theta}}^l) \rangle \\ &+ \Delta t a_{kk} \left(\partial_{xx} \hat{\boldsymbol{\Theta}}^k + \frac{\mu}{3} \partial_{xx} \mathbf{B}(\hat{\boldsymbol{\Theta}}^k) \right).\end{aligned} \tag{67}$$

Thus, $\langle \hat{\mathbf{R}}^k \rangle$ can be expressed in terms of $\hat{\boldsymbol{\Theta}}^k$ and other explicit terms. Inserting it back to (65), then

$$\begin{aligned}\hat{\boldsymbol{\Theta}}^k =& \hat{\boldsymbol{\theta}}^n + \Delta t \sum_{l=1}^{k-1} a_{kl} h(\hat{\boldsymbol{\Theta}}^l) + \Delta t a_{kk} \partial_{xx} \hat{\boldsymbol{\Theta}}^k - \frac{\Delta t a_{kk}}{\varepsilon^2} \mathbf{B}(\hat{\boldsymbol{\Theta}}^k) \\ &+ \frac{\Delta t a_{kk}}{\varepsilon^2} \left[\hat{\boldsymbol{\theta}}^n + \Delta t \sum_{l=1}^{k-1} a_{kl} h(\hat{\boldsymbol{\Theta}}^l) + \langle \hat{\mathbf{r}}^n + \Delta t \sum_{l=1}^{k-1} \tilde{a}_{kl} f_1(\hat{\mathbf{J}}^l, \hat{\boldsymbol{\Theta}}^l) + \Delta t \sum_{l=1}^{k-1} a_{kl} f_2(\hat{\mathbf{R}}^l, \hat{\boldsymbol{\Theta}}^l) \rangle \right. \\ &\left. + \Delta t a_{kk} \left(\partial_{xx} \hat{\boldsymbol{\Theta}}^k + \frac{\mu}{3} \partial_{xx} \mathbf{B}(\hat{\boldsymbol{\Theta}}^k) \right) - \hat{\boldsymbol{\Theta}}^k \right].\end{aligned} \tag{68}$$

Reorder and approximate $\mathbf{B}(\hat{\boldsymbol{\Theta}}^k)$ by $\mathbf{B}(\hat{\boldsymbol{\Theta}}^{k-1}) + 4\mathbf{C}(\hat{\boldsymbol{\Theta}}^{k-1})(\hat{\boldsymbol{\Theta}}^k - \hat{\boldsymbol{\Theta}}^{k-1})$ and $\partial_{xx} \mathbf{B}(\hat{\boldsymbol{\Theta}}^k)$ by $\partial_x (4\mathbf{C}(\hat{\boldsymbol{\Theta}}^{k-1}) \partial_x \hat{\boldsymbol{\Theta}}^k)$, one gets

$$\begin{aligned}&\left[\left(1 + \frac{\Delta t a_{kk}}{\varepsilon^2} \right) \mathbf{I} + \frac{\Delta t a_{kk}}{\varepsilon^2} 4\mathbf{C}(\hat{\boldsymbol{\Theta}}^{k-1}) \right] \hat{\boldsymbol{\Theta}}^k - \Delta t a_{kk} \left(1 + \frac{\Delta t a_{kk}}{\varepsilon^2} \right) \partial_{xx} \hat{\boldsymbol{\Theta}}^k \\ &- \frac{(\Delta t a_{kk})^2}{\varepsilon^2} \frac{4\mu}{3} \partial_x (\mathbf{C}(\hat{\boldsymbol{\Theta}}^{k-1}) \partial_x \hat{\boldsymbol{\Theta}}^k) \\ =& \left(1 + \frac{\Delta t a_{kk}}{\varepsilon^2} \right) \hat{\boldsymbol{\theta}}^n + \left(1 + \frac{\Delta t a_{kk}}{\varepsilon^2} \right) \Delta t \sum_{l=1}^{k-1} a_{kl} h(\hat{\boldsymbol{\Theta}}^l) \\ &+ \frac{\Delta t a_{kk}}{\varepsilon^2} \left[\langle \hat{\mathbf{r}}^n + \Delta t \sum_{l=1}^{k-1} \tilde{a}_{kl} f_1(\hat{\mathbf{J}}^l, \hat{\boldsymbol{\Theta}}^l) + \Delta t \sum_{l=1}^{k-1} a_{kl} f_2(\hat{\mathbf{R}}^l, \hat{\boldsymbol{\Theta}}^l) \rangle + 3\mathbf{B}(\hat{\boldsymbol{\Theta}}^{k-1}) \right],\end{aligned} \tag{69}$$

where $\mathbf{I}$ is a $K \times K$ identity matrix, $\mathbf{B}$ and $\mathbf{C}$ are the same as (57) and (59).

Following the same space discretization as in section 2.3,

$$\begin{aligned}&\left[\left(1 + \frac{\Delta t a_{kk}}{\varepsilon^2} \right) \mathbf{I} + \frac{\Delta t a_{kk}}{\varepsilon^2} 4\mathbf{C}(\hat{\boldsymbol{\Theta}})_i^k \right] \hat{\boldsymbol{\Theta}}_i^k - \Delta t a_{kk} \left(1 + \frac{\Delta t a_{kk}}{\varepsilon^2} \right) \frac{\hat{\boldsymbol{\Theta}}_{i+1}^k - 2\hat{\boldsymbol{\Theta}}_i^k + \hat{\boldsymbol{\Theta}}_{i-1}^k}{\Delta x^2} \\ &- \frac{(\Delta t a_{kk})^2}{\varepsilon^2} \frac{4\mu}{3} \frac{\mathbf{C}(\hat{\boldsymbol{\Theta}})_{i+1/2}^{k-1} (\hat{\boldsymbol{\Theta}}_{i+1}^k - \hat{\boldsymbol{\Theta}}_i^k) - \mathbf{C}(\hat{\boldsymbol{\Theta}})_{i-1/2}^{k-1} (\hat{\boldsymbol{\Theta}}_i^k - \hat{\boldsymbol{\Theta}}_{i-1}^k)}{\Delta x^2} \\ =& \left(1 + \frac{\Delta t a_{kk}}{\varepsilon^2} \right) \hat{\boldsymbol{\theta}}_i^n + \left(1 + \frac{\Delta t a_{kk}}{\varepsilon^2} \right) \Delta t \sum_{l=1}^{k-1} a_{kl} h(\hat{\boldsymbol{\Theta}}_i^l) \\ &+ \frac{\Delta t a_{kk}}{\varepsilon^2} \left[\langle \hat{\mathbf{r}}_i^n + \Delta t \sum_{l=1}^{k-1} \tilde{a}_{kl} f_1(\hat{\mathbf{J}}_i^l, \hat{\boldsymbol{\Theta}}_i^l) + \Delta t \sum_{l=1}^{k-1} a_{kl} f_2(\hat{\mathbf{R}}_i^l, \hat{\boldsymbol{\Theta}}_i^l) \rangle + 3\mathbf{B}(\hat{\boldsymbol{\Theta}}_i^{k-1}) \right],\end{aligned} \tag{70}$$

where

$$h(\hat{\mathbf{\Theta}}_i^l) = \frac{\hat{\mathbf{\Theta}}_{i+1}^l - 2\hat{\mathbf{\Theta}}_i^l + \hat{\mathbf{\Theta}}_{i-1}^l}{\Delta x^2} - \frac{1}{\varepsilon^2}(\mathbf{B}(\hat{\mathbf{\Theta}}_i^l) - \langle\hat{\mathbf{R}}_i^l\rangle),$$

$$\begin{aligned} f_1(\hat{\mathbf{J}}_i^l, \hat{\mathbf{\Theta}}_i^l) = &-\frac{v}{2\Delta x}(\hat{\mathbf{J}}_{i+1}^l - \hat{\mathbf{J}}_{i-1}^l) + \frac{v\phi^{1/2}}{2\Delta x}(\hat{\mathbf{R}}_{i+1}^l - 2\hat{\mathbf{R}}_i^l + \hat{\mathbf{R}}_{i-1}^l) \\ &- \frac{v\phi^{1/2}}{4}(\boldsymbol{\gamma}_i^l - \boldsymbol{\gamma}_{i-1}^l + \boldsymbol{\beta}_{i+1}^l - \boldsymbol{\beta}_i^l) - \frac{\mu}{3}\frac{\mathbf{B}(\hat{\mathbf{\Theta}}_{i+1}^l) - 2\mathbf{B}(\hat{\mathbf{\Theta}}_i^l) + \mathbf{B}(\hat{\mathbf{\Theta}}_{i-1}^l)}{\Delta x^2}, \end{aligned}$$

$$f_2(\hat{\mathbf{R}}_i^l, \hat{\mathbf{\Theta}}_i^l) = \frac{1}{\varepsilon^2}(\mathbf{B}(\hat{\mathbf{\Theta}}_i^l) - \hat{\mathbf{R}}_i^l) + \frac{\mu}{3}\frac{\mathbf{B}(\hat{\mathbf{\Theta}}_{i+1}^l) - 2\mathbf{B}(\hat{\mathbf{\Theta}}_i^l) + \mathbf{B}(\hat{\mathbf{\Theta}}_{i-1}^l)}{\Delta x^2},$$

with $\boldsymbol{\gamma}_i^l$ and $\boldsymbol{\beta}_i^l$ the same as (28).

We omit the details of velocity discretization and other space discretization, which is the same as in section 2.3. On the left hand side of (70), we specify the approximation of $\mathbf{C}(\hat{\mathbf{\Theta}})_{i+1/2}^{k-1}$ by

$$\mathbf{C}(\hat{\mathbf{\Theta}})_{i+1/2}^{k-1} \approx \frac{1}{2}\left(\mathbf{C}(\hat{\mathbf{\Theta}})_{i+1}^{k-1} + \mathbf{C}(\hat{\mathbf{\Theta}})_i^{k-1}\right).$$

Notice that to solve out $\hat{\mathbf{\Theta}}_i^k$, one needs to invert a large $K(N_x+1) \times K(N_x+1)$ matrix $\mathbf{M}$, where N_x+1 is the number of discretized points in space. $\mathbf{M}$ is defined as following:

$$\mathbf{M}_{Ki+1:K(i+1),Kj+1:K(j+1)} = \begin{cases} \mathbf{m}_i^1 & \text{for } j = i-1 \\ \mathbf{m}_i^2 & \text{for } j = i \\ \mathbf{m}_i^3 & \text{for } j = i+1 \\ 0 & \text{otherwise} \end{cases}, \quad i = 0, 1, \cdots, N_x \tag{71}$$

with $K \times K$ matrix $\mathbf{m}^1, \mathbf{m}^2$ and $\mathbf{m}^3$:

$$\begin{aligned} \mathbf{m}_i^1 =& -\frac{\Delta t a_{kk}}{\Delta x^2}\left(1 + \frac{\Delta t a_{kk}}{\varepsilon^2}\right)\mathbf{I} - \frac{(\Delta t a_{kk})^2}{2\varepsilon^2\Delta x^2}\frac{4\mu}{3}\left[\mathbf{C}(\hat{\mathbf{\Theta}})_{i-1}^{k-1} + \mathbf{C}(\hat{\mathbf{\Theta}})_i^{k-1}\right]; \\ \mathbf{m}_i^2 =& \left(1 + \frac{\Delta t a_{kk}}{\varepsilon^2}\right)\mathbf{I} + \frac{\Delta t a_{kk}}{\varepsilon^2}4\mathbf{C}(\hat{\mathbf{\Theta}})_i^{k-1} + \frac{2\Delta t a_{kk}}{\Delta x^2}\left(1 + \frac{\Delta t a_{kk}}{\varepsilon^2}\right)\mathbf{I} \\ &+ \frac{(\Delta t a_{kk})^2}{2\varepsilon^2\Delta x^2}\frac{4\mu}{3}\left[\mathbf{C}(\hat{\mathbf{\Theta}})_{i+1}^{k-1} + 2\mathbf{C}(\hat{\mathbf{\Theta}})_i^{k-1} + \mathbf{C}(\hat{\mathbf{\Theta}})_{i-1}^{k-1}\right]; \\ \mathbf{m}_i^3 =& -\frac{\Delta t a_{kk}}{\Delta x^2}\left(1 + \frac{\Delta t a_{kk}}{\varepsilon^2}\right)\mathbf{I} - \frac{(\Delta t a_{kk})^2}{2\varepsilon^2\Delta x^2}\frac{4\mu}{3}\left[\mathbf{C}(\hat{\mathbf{\Theta}})_i^{k-1} + \mathbf{C}(\hat{\mathbf{\Theta}})_{i+1}^{k-1}\right]. \end{aligned} \tag{72}$$

From [19], one can prove the matrix $\left(1 + \frac{\Delta t a_{kk}}{\varepsilon^2}\right)\mathbf{I} + \frac{\Delta t a_{kk}}{\varepsilon^2}4\mathbf{C}(\hat{\mathbf{\Theta}})_i^{k-1}$ is symmetric, positive and definite under some gentle conditions. Then obviously, $\mathbf{M}$ is strictly block diagonal dominant, thus invertible. Since $\mathbf{M}$ is also sparse, fast algorithm can be applied to solve $\hat{\mathbf{\Theta}}^k$, then $\hat{\mathbf{R}}^k$ and $\hat{\mathbf{J}}^k$ can be obtained from (64a) and (64b) subsequently.

3.4 The sAP Property

Similar as in section 2.4, setting $\varepsilon \to 0$ in (64), one gets

$$\hat{\mathbf{R}}_i^k = \mathbf{B}(\hat{\mathbf{\Theta}}_i^k), \tag{73a}$$

$$\hat{\mathbf{J}}_i^k = -v\frac{\hat{\mathbf{R}}_{i+1}^k - \hat{\mathbf{R}}_{i-1}^k}{2\Delta x}, \tag{73b}$$

$$\langle\hat{\mathbf{R}}_i^k\rangle = \mathbf{B}(\hat{\mathbf{\Theta}}_i^k). \tag{73c}$$

Inserting (73) back into (63a) + (63c) and setting $\varepsilon = 0$,

$$\hat{\mathbf{r}}_i^{n+1} + \hat{\boldsymbol{\theta}}_i^{n+1} = \hat{\mathbf{r}}_i^n + \hat{\boldsymbol{\theta}}_i^n + \Delta t \sum_{k=1}^{s} \tilde{b}_k \hat{f}_1(\hat{\mathbf{R}}_i^k, \hat{\boldsymbol{\Theta}}_i^k) + \Delta t \sum_{k=1}^{s} b_k \hat{f}_2(\hat{\mathbf{R}}_i^k, \hat{\boldsymbol{\Theta}}_i^k) + \Delta t \sum_{k=1}^{s} b_k \hat{h}(\hat{\boldsymbol{\Theta}}_i^k), \tag{74}$$

where

$$\hat{f}_1(\hat{\mathbf{R}}^k, \hat{\boldsymbol{\Theta}}^k) = v^2 \frac{\hat{\mathbf{R}}_{i+2}^k - 2\hat{\mathbf{R}}_i^k + \hat{\mathbf{R}}_{i-2}^k}{4\Delta x^2} - \frac{\mathbf{B}(\hat{\boldsymbol{\Theta}}_{i+1}^k) - 2\mathbf{B}(\hat{\boldsymbol{\Theta}}_i^k) + \mathbf{B}(\hat{\boldsymbol{\Theta}}_{i-1}^k)}{3\Delta x^2}, \tag{75a}$$

$$\hat{f}_2(\hat{\boldsymbol{\Theta}}^k) = \frac{\mathbf{B}(\hat{\boldsymbol{\Theta}}_{i+1}^k) - 2\mathbf{B}(\hat{\boldsymbol{\Theta}}_i^k) + \mathbf{B}(\hat{\boldsymbol{\Theta}}_{i-1}^k)}{3\Delta x^2}, \tag{75b}$$

$$\hat{h}(\hat{\boldsymbol{\Theta}}^k) = \frac{\hat{\boldsymbol{\Theta}}_{i+1}^k - 2\hat{\boldsymbol{\Theta}}_i^k + \hat{\boldsymbol{\Theta}}_{i-1}^k}{\Delta x^2}. \tag{75c}$$

Take $\langle\cdot\rangle$ on (74) and use (73c),

$$\begin{aligned} \hat{\boldsymbol{\theta}}_i^{n+1} + \mathbf{B}(\hat{\boldsymbol{\theta}}_i^{n+1}) =& \hat{\boldsymbol{\theta}}_i^n + \mathbf{B}(\hat{\boldsymbol{\theta}}_i^n) + \Delta t \sum_{k=1}^{s} b_k \left[\frac{\hat{\boldsymbol{\Theta}}_{i+1}^k - 2\hat{\boldsymbol{\Theta}}_i^k + \hat{\boldsymbol{\Theta}}_{i-1}^k}{\Delta x^2} \right. \\ & \left. + \frac{\mathbf{B}(\hat{\boldsymbol{\Theta}}_{i+1}^k) - 2\mathbf{B}(\hat{\boldsymbol{\Theta}}_i^k) + \mathbf{B}(\hat{\boldsymbol{\Theta}}_{i-1}^k)}{3\Delta x^2} \right] + O(\Delta x^2), \end{aligned} \tag{76}$$

where

$$\begin{aligned} \hat{\boldsymbol{\Theta}}_i^k + \mathbf{B}(\hat{\boldsymbol{\Theta}}_i^k) =& \hat{\boldsymbol{\theta}}_i^n + \mathbf{B}(\hat{\boldsymbol{\theta}}_i^n) + \Delta t \sum_{l=1}^{k} a_{kl} \left[\frac{\hat{\boldsymbol{\Theta}}_{i+1}^l - 2\hat{\boldsymbol{\Theta}}_i^l + \hat{\boldsymbol{\Theta}}_{i-1}^l}{\Delta x^2} \right. \\ & \left. + \frac{\mathbf{B}(\hat{\boldsymbol{\Theta}}_{i+1}^l) - 2\mathbf{B}(\hat{\boldsymbol{\Theta}}_i^l) + \mathbf{B}(\hat{\boldsymbol{\Theta}}_{i-1}^l)}{3\Delta x^2} \right], \end{aligned} \tag{77}$$

which is an *implicit* R-K method for the limiting diffusion equation (58). Thus the sAP property is illustrated.

4 Numerical Tests

In this section we present several numerical tests to illustrate the performance of the new sAP IMEX schemes. We use notations SSP2 to denote the new scheme based on the second order IMEX-RK tableu (24) and JPT to denote the second order scheme in [20]. First we test the new approach in the deterministic case and then we consider the presence of uncertainties.

4.1 Test 1: The Linear Transport Equation

We consider problem (1) with

$$x \in [0,1],\ F_L(v) = 1,\ F_R(v) = 0,\ \sigma_s = 1,\ \sigma_A = 0,\ Q = 0,\ \varepsilon = 10^{-6}$$

We reported the results at different time $t = 0.01, t = 0.05$ and $t = 0.15$ in Figure 1. In all figures we use notations NT to denote the number of time iterations. With fixed $\Delta x = 0.01$, for JPT ($\circ$) $\Delta t = 0.5(\Delta x)^2$, $NT = 200, 1000, 3000$; for SSP2 ($\diamond$) $\Delta t = \lambda \Delta x$ with $\lambda = 0.04$, $NT = 25, 125, 375$. The exact diffusive solution is computed by equation (2) with the same mesh size in dashed line. One can see that both methods are AP and work well in the diffusive regime at any times. The time cost of the two methods are reported in Table 1, which shows that SSP2 is about 7 times more efficient than JPT.

	$t = 0.01$	$t = 0.05$	$t = 0.15$
JPT	0.451567s	2.014770s	6.069805s
SSP2	0.069801s	0.290240s	0.815041s

Table 1: Test 1. Time cost comparison in seconds between JPT and SSP2 schemes.

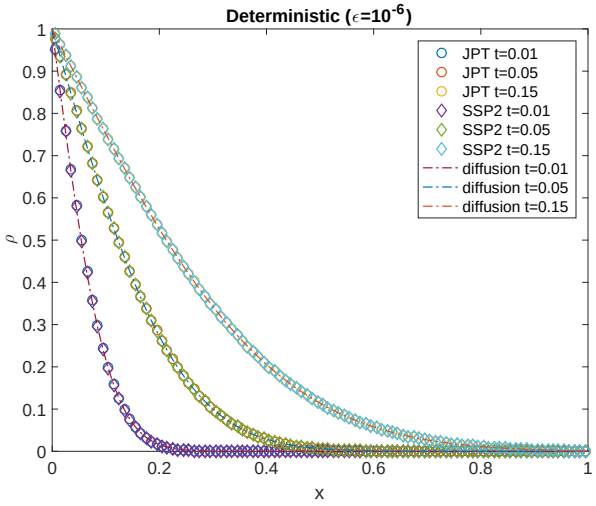

Figure 1: Test 1. The solution of the mass density ρ to the linear transport equation. JPT ($\circ$), $\Delta x = 0.01$, $\Delta t = 0.5(\Delta x)^2$, $NT = 200, 1000, 3000$; SSP2 ($\diamond$), $\Delta x = 0.01$, $\Delta t = \lambda \Delta x$ with $\lambda = 0.04$, $NT = 25, 125, 375$.

4.2 Test 2: The Linear Transport Equation with Random Inputs

We consider problem (1) with random inputs and

$$x \in [0, 1],\ F_L(v) = 1,\ F_R(v) = 0,\ \sigma_s = 1 + 0.5z,\ \sigma_A = 0,\ Q = 0,\ \varepsilon = 10^{-6},$$

where z follows uniform distribution on $[-1, 1]$ (Denoted by $z \sim \mathcal{U}[-1, 1]$ in the following tests).

The mean and standard deviation are two quantities of our interest. So we examine these two quantities of the numerical solutions at different time $t = 0.01, t = 0.05$ and $t = 0.15$ in Figure 2. Given the gPC coefficients $\hat{\rho}_k$ of ρ, it's convenient to calculate the mean value and standard deviation by

$$\mathrm{E}[\rho] \approx \hat{\rho}_1,\ \mathrm{Sd}[\rho] \approx \sqrt{\sum_{k=2}^{K} \hat{\rho}_k^2}.$$

With fixed $\Delta x = 0.025$, for JPT ($\circ$) $\Delta t = 0.0002$ and $NT = 50, 250, 750$; for SSP2 ($\diamond$) $\Delta t = \lambda \Delta x$ with $\lambda = 0.035$, $NT = 11, 57, 171$. The exact diffusive solution is represented by the dashed line. As expected, both methods are sAP and match well in the diffusive regime at any times. The distribution of $\rho(x, z)$ at different times are presented in Figure 3. We report the time cost comparison of gPC-JPT and gPC-SSP2 in Table 2, which shows that gPC-SSP2 is more than 3 times faster than gPC-JPT. Since randomness is introduced and computation becomes more time-consuming, the efficiency of gPC-SSP2 is remarkable.

	$t = 0.01$	$t = 0.05$	$t = 0.15$
gPC-JPT	2.662382s	13.159598s	39.255826s
gPC-SSP2	0.759259s	3.865332s	11.424931s

Table 2: Test 2. Time cost comparison in seconds between JPT and SSP2 schemes.

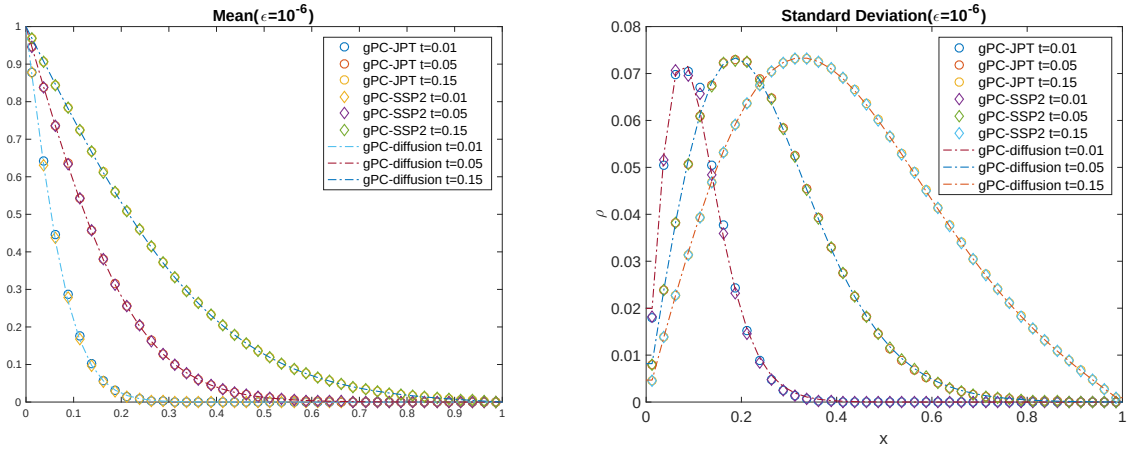

Figure 2: Test 2. The mean (left) and standard deviation (right) of the solution of the mass density ρ to the linear transport equation. JPT ($\circ$), $\Delta x = 0.025$, $\Delta t = 0.0002$, $NT = 50, 250, 750$; SSP2 ($\diamond$), $\Delta x = 0.025$, $\Delta t = \lambda \Delta x$ with $\lambda = 0.035$, $NT = 11, 57, 171$.

4.3 Test 3: The Radiative Heat Transfer Equation

We then compare the two methods for deterministic radiative heat transfer equations (44) near diffusive regime ($\varepsilon = 10^{-6}$) with the following initial and boundary conditions:

$$
\begin{aligned}
&I_I(x, \mu, z, 0) = 0, \quad \theta_I(x, z, 0) = 0, \quad x \in [0, 1] \\
&\theta_B(0, z, t) = 1, \ \theta_B(1, z, t) = 0; \\
&I_B(0, \mu, z, t) = 1, \ \mu > 0, \quad I_B(1, \mu, z, t) = 0, \ \mu < 0,
\end{aligned}
$$

and constant coefficient

$$\sigma(x) = 1.$$

Figure 4 shows the solutions of temperature θ at different time $t = 0.01, t = 0.05$ and $t = 0.15$. With fixed $\Delta x = 0.025$, for JPT ($\circ$) $\Delta t = 0.002$; for SSP2 ($\diamond$) $\Delta t = \lambda \Delta x$ with $\lambda = 0.035$. The exact diffusive solution is computed by equation (53) with the same mesh size in dashed line. One can see that both methods are AP and work well in the diffusive regime at any times. The time cost of both methods are reported in Table 3, which shows that SSP2 is about twice times faster than JPT in this nonlinear case.

	$t = 0.01$	$t = 0.05$	$t = 0.15$
JPT	0.112507s	0.268415s	0.806410s
SSP2	0.059658s	0.208812s	0.583166s

Table 3: Test 3. Time cost comparison in seconds between JPT and SSP2 schemes.

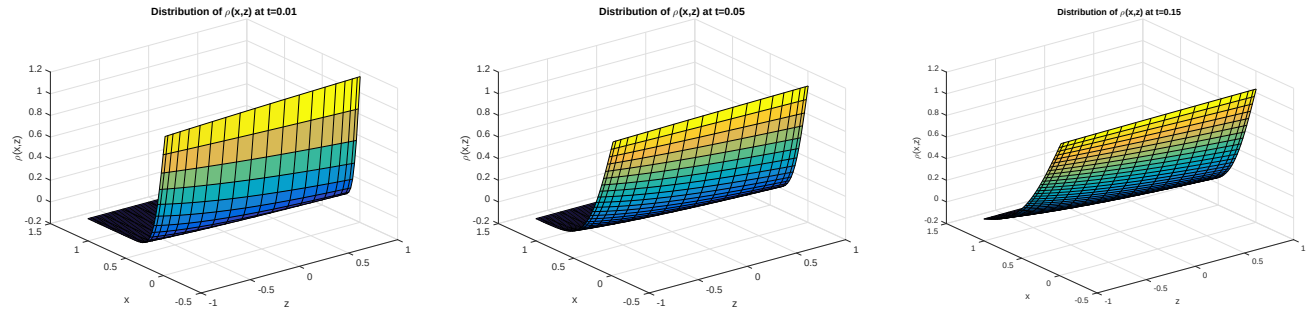

Figure 3: Test 2. Distribution of the mass density $\rho(x, z)$ to the linear transport equation by gPC-SSP2 with $NT = 11, 57, 171$.

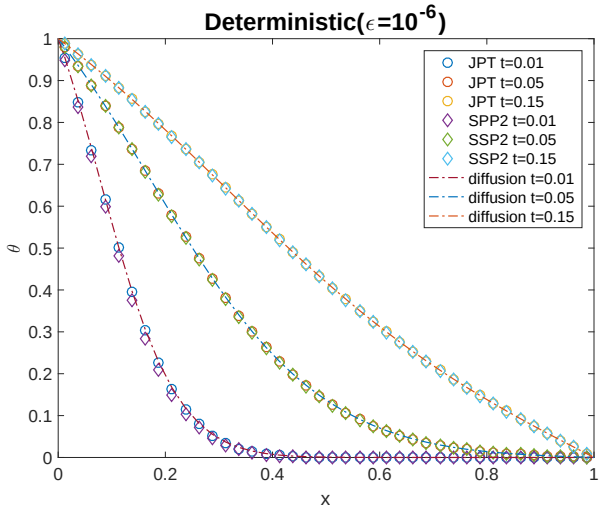

Figure 4: Test 3. The solution of the temperature θ to the radiative heat transfer equation. JPT ($\circ$), $\Delta x = 0.025$, $\Delta t = 0.0002$, $NT = 50, 250, 750$; SSP2 ($\diamond$), $\Delta x = 0.025$, $\Delta t = \lambda \Delta x$ with $\lambda = 0.035$, $NT = 11, 57, 171$.

4.4 Test 4: The Radiative Heat Transfer Equation with Random Inputs

We then compare the two methods in the equations (44) with randomness in the cross-section with the following initial and boundary conditions:

$$
\begin{aligned}
&I_I(x, \mu, z, 0) = 0, \quad \theta_I(x, z, 0) = 0, \quad x \in [0, 1] \\
&\theta_B(0, z, t) = 1, \ \theta_B(1, z, t) = 0; \\
&I_B(0, \mu, z, t) = 1 + 0.5z, \ \mu > 0, \quad I_B(1, \mu, z, t) = 0, \ \mu < 0,
\end{aligned}
$$

and random coefficient

$$\sigma(z) = 1 + 0.5z, \ z \sim \mathcal{U}[-1, 1].$$

In Figure 5, we report the mean and standard deviation of the temperature θ at different time $t = 0.01, t = 0.05$ and $t = 0.15$. Similar to Test 2, the mean value and standard deviation are calculated

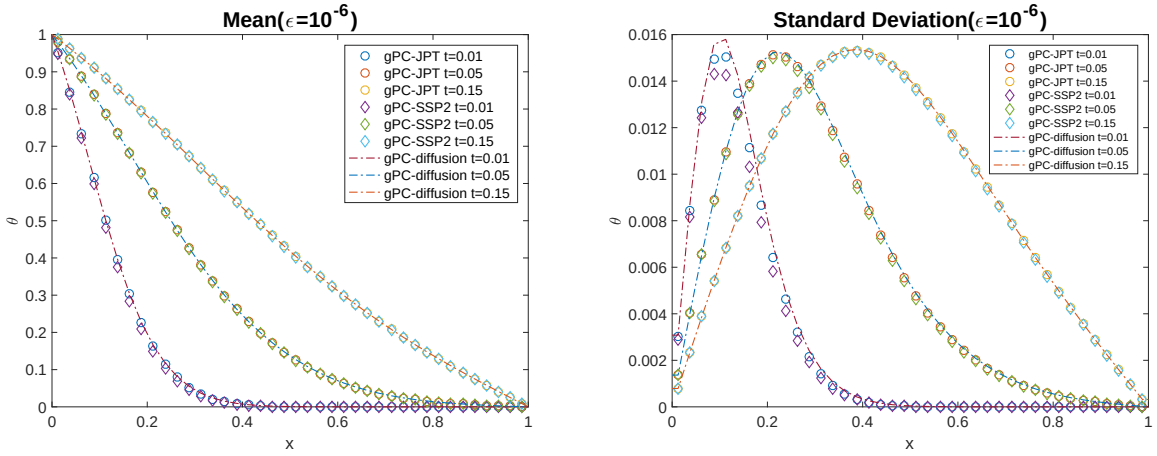

Figure 5: Test 4. The mean (left) and standard deviation (right) of the solution of the temperature θ to the radiative heat transfer equation. JPT ($\circ$), $\Delta x = 0.025$, $\Delta t = 0.0002$, $NT = 50, 250, 750$; SSP2 ($\diamond$), $\Delta x = 0.025$, $\Delta t = \lambda \Delta x$ with $\lambda = 0.035$, $NT = 11, 57, 171$.

by

$$\mathrm{E}[\theta] \approx \hat{\theta}_1, \ \mathrm{Sd}[\theta] \approx \sqrt{\sum_{k=2}^{K} \hat{\theta}_k^2}.$$

With fixed $\Delta x = 0.025$, for JPT ($\circ$) $\Delta t = 0.0002$ and $NT = 50, 250, 750$; for SSP2 ($\diamond$) $\Delta t = \lambda \Delta x$ with $\lambda = 0.035$, $NT = 11, 57, 171$. The reference diffusive solution is represented by the dashed line. We refer to [19] for the same results using micro-macro decomposition based gPC method. Good agreements of gPC-JPT, gPC-SSP2 methods and reference solution are observed in the diffusive regime at any time. The distribution of $\theta(x, z)$ at different times are presented in Figure 6. We report the time cost comparison of gPC-JPT and gPC-SSP2 in Table 4, which shows that gPC-SSP2 is nearly 4 times faster than gPC-JPT. The nonlinearity slows down gPC-JPT a lot and thus the advantage in efficiency of gPC-SSP2 is significant in this nonlinear problem with random inputs.

	$t = 0.01$	$t = 0.05$	$t = 0.15$
gPC-JPT	172.431508s	804.915170s	2329.405654s
gPC-SSP2	36.945166s	192.040137s	626.736282s

Table 4: Test 4. Time cost comparison in seconds between JPT and SSP2 schemes.

5 Conclusions

In this article, for linear transport and radiative heat transfer equations with random inputs, new generalized polynomial chaos based Asymptotic-Preserving stochastic Galerkin schemes are introduced. Compared with previous methods for these problems, our new method use the implicit-explicit (IMEX) time discretization to gain higher order accuracy, and by using a modified diffusion operator based penalty method, a more relaxed stability condition–a hyperbolic, rather than parabolic, CFL condition–is achieved when mean free path is small, in the diffusive regime.

These schemes allow efficient computation of random transport equations that contain both uncertainties and multiscales, allowing Knudsen number independent time step, mesh size and degree of

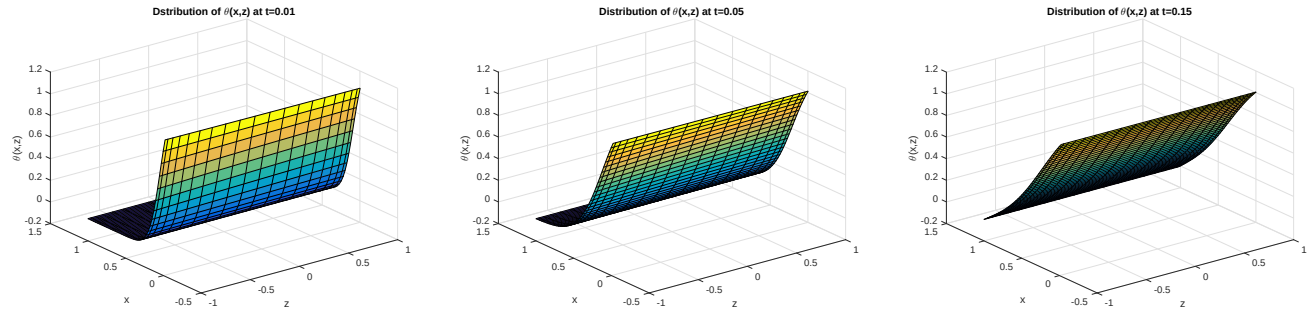

Figure 6: Test 2. Distribution of the temperature $\theta(x, z)$ to the radiative heat transfer equation by gPC-SSP2 with $NT = 11, 57, 171$.

polynomials, with a spectral accuracy in the random space.They can be used efficiently for all range of Knudsen numbers.

There remain many issues to be resolved. First, we only studied one dimensional problem in space and velocity. The next step will be to extend the methods to high dimensions. In addition, multi-dimensional challenge is also presented in the random space. Sparse grids could be used, as was done in [32], but it remains to be explored.

References

[1] C. Bardos, R. Santos, and R. Sentis, Diffusion approximation and computation of the critical size. Trans. Amer. Math. Soc., 284, 617–649, 1984.

[2] S. Boscarino, L. Pareschi, and G. Russo, Implicit-explicit Runge–Kutta schemes for hyperbolic systems and kinetic equations in the diffusion limit. SIAM Journal on Scientific Computing, 35(1):A22–A51, 2013.

[3] S. Boscarino, L. Pareschi, and G. Russo, A unified IMEX Runge-Kutta approach for hyperbolic systems with multiscale relaxation. *Preprint*, 2017.

[4] F. Bouchut, F. Golse and M. Pulvirenti, Kinetic Equations and Asymptotic Theory. Seriers in Applied Math., Ed. B. Perthame and L. Desvillettes, Elsevier, 2000.

[5] C. Buet, S. Cordier, An asymptotic preserving scheme for hydrodynamics radiative transfer models, Numerische Math. 108, 2, 199–221, 2007.

[6] J.A. Carrillo, T. Goudon, P. Lafitte, F. Vecil, Numerical schemes of diffusion asymptotics and moment closures for kinetic equations. J. Sci. Comput., 36, 113-149, 2008.

[7] Z. Chen, L. Liu, and L. Mu, DG-IMEX Stochastic Galerkin schemes for Linear Transport Equation with Random Inputs and Diffusive Scalings. *Preprint*, 2016.

[8] K.M. Case, P.F. Zweifel, Linear Transport Theory. Addison-Wesley, Reading, MA, 1997.

[9] F. Cavalli, G. Naldi, G. Puppo, M. Semplice, High order relaxation schemes for non linear diffusion problems. SIAM Journal on Numerical Analysis, 45 2098-2119, 2007.

[10] S. Chandrasekhar, Radiative Transport. Dover, New York, 1960.

[11] P. Degond, Asymptotic-preserving schemes for fluid models of plasmas. In Numerical models for fusion, volume 39/40 of Panor. Syntheses, pages 1–90. Soc. Math. France, Paris, 2013.

[12] P. Degond and F. Deluzet, Asymptotic-preserving methods and multiscale models for plasma physics. J. Comp. Phys., 2017 (to appear).

[13] G. Dimarco, L. Pareschi, Numerical methods for kinetic equations, Acta Numerica 23, 369–520, 2014.

[14] L. Gosse, G. Toscani, Asymptotic-preserving and well-balanced schemes for radiative transfer and the Rosseland approximation. Numer. Math., 98, 2, 223–250, 2004.

[15] J. Hu and S. Jin, A stochastic Galerkin method for the Boltzmann equation with uncertainty , J. Comp. Phys. 315, 150–168, 2016.

[16] S. Jin, Asymptotic preserving (AP) schemes for multiscale kinetic and hyperbolic equations: a review. Lecture Notes for Summer School on Methods and Models of Kinetic Theory (M&MKT), Porto Ercole (Grosseto, Italy), 177–216, 2010.

[17] S. Jin, J.-G. Liu and Z. Ma, Uniform spectral convergence of the stochastic Galerkin method for the linear transport equations with random inputs in diffusive regime and a micro-macro decomposition based asymptotic preserving method. Research in Math. Sci., to appear.

[18] S. Jin and L. Liu, An Asymptotic-Preserving Stochastic Galerkin Method for the semiconductor Boltzmann equation with random inputs and diffusive scalings, Multiscale Model. Simul. 15, 157-183, 2017.

[19] S. Jin and H. Lu, An asymptotic-preserving stochastic Galerkin method for the radiative heat transfer equations with random inputs and diffusive scalings. J. Comp. Phys. 334, 182–206, 2017.

[20] S. Jin, L. Pareschi, and G. Toscani, Uniformly accurate diffusive relaxation schemes for multiscale transport equations. SIAM J. Num. Anal., 38(3),913–936, 2000.

[21] S. Jin, D. Xiu, and X. Zhu, Asymptotic-preserving methods for hyperbolic and transport equations with random inputs and diffusive scalings. J. Comp. Phys., 289, 35–52, 2015.

[22] A. Klar, An asymptotic-induced scheme for nonstationary transport equations in the diffusive limit. SIAM J. Numer. Anal., 35, 1073–1094, 1998.

[23] A. Klar and C. Schmeiser, Numerical passage from radiative heat transfer to nonlinear diffusion models. Math. Models Methods Appl. Sci., 11, 749–767, 2001.

[24] P. Lafitte, G. Samaey, Asymptotic-preserving projective integration schemes for kinetic equations in the diffusion limit, SIAM J. Sci. Comput., 34(2), A579–A602. 2012.

[25] E.W. Larsen and J. B. Keller, Asymptotic solution of neutron transport problems for small mean free paths. J. Math. Phys., 15, 75–81, 1974.

[26] E.W. Larsen and J. E. Morel, Asymptotic solutions of numerical transport problems in optically thick, diffusive regimes. II. J. Comput. Phys., 83, 212–236, 1989.

[27] E.W. Larsen, J. E. Morel, and W.F. Miller, Jr., Asymptotic solutions of numerical transport problems in optically thick, diffusive regimes. J. Comput. Phys., 69, 283–324, 1987.

[28] M. Lemou, L. Mieussens, A new asymptotic preserving scheme based on micro-macro formulation for linear kinetic equations in the diffusion limit. SIAM J. Sci. Comp. 31, 334–368, 2010.

[29] Q. Li and L. Wang, Uniform regularity for linear kinetic equations with random input based on hypocoercivity, preprint. ArXiv: 1612.01219.

[30] G. Naldi, L. Pareschi, Numerical schemes for hyperbolic systems of conservation laws with stiff diffusive relaxation, SIAM J. Num. Anal., 37, 1246–1270, 2000.

[31] L. Pareschi, G. Russo, Implicit-Explicit Runge-Kutta schemes and applications to hyperbolic systems with relaxations. J. Sci. Comp. 25, 129–155, 2005.

[32] R. Shu, J. Hu and S. Jin, A stochastic Galerkin method for the Boltzmann equation with high dimensional random inputs using sparse grids. *Preprint*, 2016.

[33] H. Spohn, Large Scale Dynamics of Interacting Particles, Springer-Verlag, 1991.

[34] W. Sun, S. Jiang, and K. Xu, An asymptotic preserving unified gas kinetic scheme for gray radiative transfer equations. J. Comput. Phys., 285, 265–279, 2015.

[35] Y. Zhu and S. Jin, The Vlasov-Poisson-Fokker-Planck system with uncertainty and a one-dimensional asymptotic-preserving method. *Preprint*, 2016.